Production of electricity and hydrogen by photocatalytic degradation of organic wastes in a photoelectrochemical cell
The concept of the Photofuelcell: A review of a re-emerging research field

Panagiotis Lianos*

Engineering Science Deptartment, University of Patras, 26500 Patras, Greece

ARTICLE INFO

ABSTRACT

The present review aims to give to a researcher who has no experience with Photofuelcells all necessary basic knowledge to join the field without much trouble and to give to an experienced researcher a handy manual of reference. The author has dealt with the principal matters related with the design of a photoelectrochemical cell and the factors that affect efficient production of electricity by photocatalytic degradation of (principally) organic and (secondarily) inorganic waste materials. A large portion of the paper is devoted to the review of materials used for making a photoanode since most of the accomplished research is on this exact matter. The paper also briefly reviews the materials used to make the rest of the components of the cell as well as the models of cell efficiency and photodegradation procedures during cell operation.

© 2010 Elsevier B.V. All rights reserved.

Contents

1. Introduction

Production of electricity and hydrogen by photocatalytic degradation of organic wastes in a photoelectrochemical (PEC) cell is an attractive project with double environmental benefit: waste material can be consumed and solar radiation can be converted into useful forms of energy, such as electricity and hydrogen. This idea is not new but a large re-emerging interest is recently expressed. Photocatalytic hydrogen production by photodegradation of organic wastes is shadowed by the more popular idea of water splitting. In fact, these two matters are studied in parallel while the basic photocatalytic setups are similar, so that in essence, they constitute one single field of research and they have the same origins. The most celebrated scientific publication that affected the development of the field was the work by Fujishima and Honda [1] in 1972, describing photocatalytic water splitting in a PEC cell using a semiconductor (rutile single crystal) electrode. This work has been the point of reference for many later research efforts [2–10], including the recent ones [11–17]. Since then, a huge amount of research has been published. After the original excitement, interest has later somehow faded [18]. However, the broad experience accumulated for more than 30 years of studies on photocatalytic degradation of organic substances [19–46], the development of new nanostructured photocatalysts, the optimization of methods of material deposition and, generally, the impressive progress of Materials Science in combination with the increasing awareness on the environmental issues have created new excitement about this field. The present review does not intend to cover all related published works but to focus on some characteristic publications and to mark the major tendencies so as to offer to readers an easy to grasp but integral view of the field.

2. Definitions

Production of hydrogen by degradation of organic substances in the presence of a photocatalyst can be distinguished into two major categories:

(1) *Photocatalytic (PC) production of hydrogen*: By this term, we usually mean production of hydrogen by heterogeneous photocatalysis using powdered or supported, pure or combined photocatalysts. As shown in Fig. 1A, the photocatalyst is excited by absorption of photons, which create electron–hole pairs. Holes oxidize the photodegradable substance, either directly or through radical intermediates, typically OH•, which are very efficient hole scavengers. Oxidation liberates hydrogen ions, which can be reduced by photogenerated electrons producing molecular hydrogen [9,19,43,47–59]. The photodegradable substance can simply be water itself; however, the product of oxidation of water is oxygen, which interacts with hydrogen regenerating water. Thus it is difficult to produce hydrogen by photocatalytic water splitting, since hydrogen and oxygen must be spatially separated. This can be only managed in a PEC cell, as it will be explained below. As a matter of fact, in order to detect photocatalytically produced hydrogen, it is necessary to apply conditions of absence of oxygen. Thus photocatalytic production of hydrogen is usually monitored by inert gas flow [56,58,59]. Photocatalytic production of hydrogen, in the above sense, will not be the main focus of the present paper.

(2) *Photoelectrochemical production of hydrogen*: In this case, hydrogen is produced in a PEC cell. The following three components are the main components of a PEC cell: (a) The anode electrode, which carries the photocatalyst and thus it is usually named "Photoanode". When the photocatalyst is an n-type semiconductor, which is almost the exclusive case, the photoanode produces electrons, i.e. it is the negative electrode. Oxidation reactions take place at the photoanode; (b) The cathode electrode, which carries the electrocatalyst, i.e. a material, which facilitates transfer of electrons from the cathode to the liquid phase. Reductive interactions take place at the (dark) cathode, for example, reduction of hydrogen ions to molecular hydrogen; (c) The electrolyte, which is added in order to increase conductivity and define the pH. The photoelectrochemical production of hydrogen is schematically illustrated in Fig. 1B. Photons are absorbed by the photoanode generating electron–hole pairs. Holes oxidize the photodegradable substance, as above, liberating hydrogen ions, which diffuse in the liquid phase. Electrons are channelled through an external circuit towards the cathode, where they reduce hydrogen ions producing hydrogen molecules [11]. Thus production of hydrogen is accompanied by flow of electrons, i.e. an electric current, in the external circuit. Hydrogen, of course, is detected in the absence of oxygen. Otherwise, in its presence, hydrogen is retained regenerating water. Water splitting in a PEC cell leads to hydrogen production, since the oxidation site, i.e. the photoanode, is spatially separated from the reduction site (cathode), thus O_2 and H_2 can be easily separated [11,12,15].

2.1. The Photofuelcell

In the presence of oxygen, for example, aerated liquid phase, no hydrogen can be detected. In that case, current can still flow in the external circuit of the PEC cell. Electrons arriving at the cathode reduce O_2 (cf. Section 3). Then the cell acts as a Photofuelcell (PFC). This term, in this or in slightly modified form, is recently gaining more and more ground [13,14,17,60–64]. A PFC consumes an
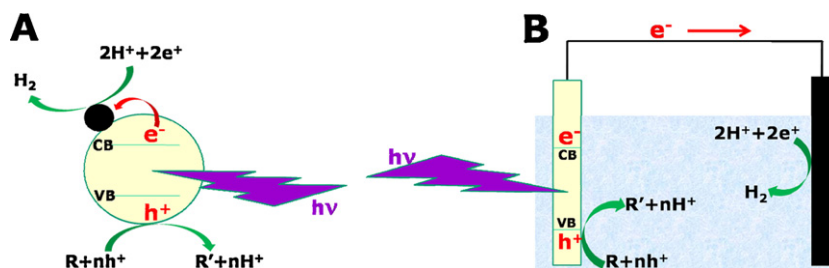
Fig. 1. Schematic representation of the photocatalytic (A) and the photoelectrochemical (B) production of hydrogen. The black full circle in (A) represents a co-catalyst (usually, a noble metal nanoparticle). The co-catalyst scavenges photogenerated electrons. In (B), anode electrode is on the left side and cathode on the right side. Oxidation and reduction may only take place when the photogenerated electron-hole pairs possess the necessary oxidation/reduction potential.
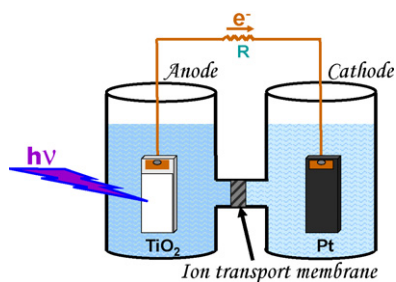
Fig. 2. Schematic representation of an H-shaped PEC cell with a TiO$_2$ anode and a Pt cathode, divided into two compartments by an ion-transport membrane. The current flows through an external load of resistance R.

Fig. 3. Schematic representation of the polarity of an external electric bias for a PEC cell.

organic substance, i.e. the fuel, and utilizes light energy to produce electricity. The present work pays special attention to PFCs, which carry promise for future applications.

3. Basic configuration of a PEC cell

The basic configuration of a PEC cell has not changed through the years, as it is seen in several publications (for example, Refs. [1,6,9,11–13,15,17,18,61–67]). It is schematically shown in Fig. 1B and Fig. 2. The cell comprises a photoanode that carries a semiconductor photocatalyst, a (dark) cathode that carries the electrocatalyst and the liquid phase that carries an electrolyte. Anode and cathode are connected through an external load. When the photocatalyst is an n-type semiconductor and the electrocatalyst is a noble metal, as it is the usual case, the photoanode acts as the negative electrode and the cathode as the positive electrode, i.e. electrons move from the anode to the cathode. The direction of the external current, of course, depends on the electric potential of each electrode. The electrochemistry of a PEC cell is fairly complicated. However, even an inexperienced experimenter can make a cell run by taking into account the following elementary considerations. When the cathode is in contact with an aqueous electrolyte at zero pH, its potential depends on the presence or absence of oxygen. In the absence of oxygen, cathode behaves as a hydrogen electrode, the potential of which is conventionally taken equal to zero. In the presence of oxygen, the cathode behaves as an oxygen electrode. Its potential is then affected by the following reductive reactions [61]:

$$O_2 + 4H^+ + 4e^- \rightarrow 2H_2O \, (+1.23 \, V) \tag{I}$$

$$O_2 + 2H^+ + 2e^- \rightarrow H_2O_2 \, (+0.68 \, V) \tag{II}$$
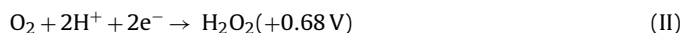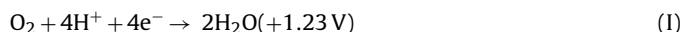
This means that its value is between 0.68 and 1.23 V. The potential of the anode depends on the Fermi level of the semiconductor photocatalyst. In the case, for example, of titania, which is the most usual case, the conduction band at zero pH has a potential, which is slightly positive and when excited it becomes slightly negative [11]. In the absence of oxygen, taking into account also the unavoidable losses, this potential difference is too weak to make the cell run spontaneously. Therefore, an external electric bias is required. By bias is meant an external electric potential, which is added between the two electrodes, as in Fig. 3, in order to increase the electromotive force driving electrons from the anode to the cathode [9]. Indeed, in such cases, various possibilities of additional bias have been proposed, the most notable ones being those where the additional voltage is provided by renewable energy devices, like photovoltaic cells (cf. [11,68–70]). In the presence of oxygen, no bias is required, since in that case a potential difference of several hundreds of mV between the two electrodes could be obtained without much of an effort [71]. Thus the Photofuelcells, which function in the presence of oxygen, are spontaneously running devices. The above electrode potentials, as already said, correspond to zero
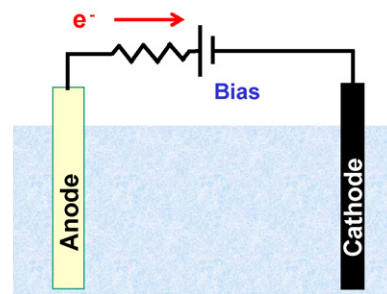
pH value. At higher pH and at room temperature, the potential of both electrodes drops according to the following equation [11]:

$$\Delta V(\text{Volts}) = -0.059x(\Delta \text{pH}). \tag{1}$$

Thus if the pH increases by the same amount for the whole liquid phase of the cell, the variation of the potential of both electrodes is the same, so the difference between the electric potential of the two electrodes remains the same. If the pH of the electrolyte around the anode is basic and that around the cathode is acidic, then the potential difference between the two electrodes increases. In that case, we say that the cell functions under chemical bias. The potential difference between the two electrodes reflects on the measured open-circuit voltage V_{oc} of the cell, which corresponds to infinite resistance R in Fig. 2. Thus V_{oc} can be much larger than 1.0 V, when chemical bias is applied. Chemical bias can be applied when the cell is structured into two compartments (as in Fig. 2) communicating through an ion-transport membrane, for example, proton-transporting Nafion membrane. However, chemical bias is not a self-sustainable situation since chemical reagents must be continuously added in the two compartments to keep pH difference, which is otherwise eventually removed by ion transport through the membrane. Further chemical bias is offered to the system when a fuel, i.e. a sacrificial agent that retains photogenerated holes, is added to the cell. In that case, the consumption of holes increases the number of photogenerated free electrons that makes anode potential more electronegative. This electric-potential variation reflects on the increase of the V_{oc} of the cell. Indeed, in a cell running with the same pH value in the anode and the cathode compartment, in the presence of ethanol or glycerol V_{oc} becomes about 0.3 V larger [71]. The above discussion shows that it is very easy to run a PFC both with and without fuel, simply by shining light on the photoanode. It is understood that this light must contain the appropriate wavelengths necessary to excite the photocatalyst.

4. Materials usually employed to make a PEC cell

As already said, the main components of a PEC cell is the photoanode, the (dark) cathode and the electrolyte. In this chapter, the most commonly used materials to make these components are reviewed.

4.1. Photoanode

A photoanode is typically made of an electrode on which a nanocrystalline semiconductor film is deposited. In the vast majority of cases, nanocrystalline titania is the preferred semiconductor photocatalyst. Indeed, titania has established itself as the so far most successful photocatalyst for heterogeneous photocatalytic degradation of organic wastes. The reason for this success is that titania is stable in most chemical environments and it can be easily synthesized and deposited as thin mesoporous film by soft-
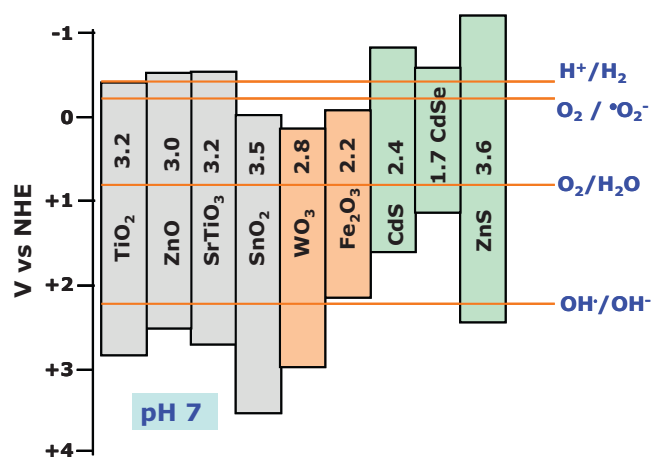
Fig. 4. E_g values (in eV) and position of CB and VB for various semiconductors at pH 7 vs. NHE. The diagram was adapted to data from previous publications [74,93–96].

chemistry techniques, like the sol–gel process. In addition, it is commercially available at very reasonable prices. Titania is used as white pigment in all kinds of products, ranging from paints to tooth pastes. For this reason, some people also stress its lack of toxicity. However, it is so far not clear whether nanoparticles are non-toxic or toxic, therefore, one should be mindful on this matter. Titania has survived despite its disadvantages, namely, the fact that it absorbs only UV radiation, which makes only a small percentage of the solar radiation at the surface of the Earth. In addition, electron–hole recombination is extensive in nanocrystalline titania, therefore techniques, which lead to electron–hole separation are necessary in order to increase cell efficiency. More on this matter will be discussed below.

4.1.1. Electrodes for photoanodes

In most cases, a transparent conductive oxide (TCO) electrode made of glass carrying a thin transparent electroconductive layer of Indium-tin-oxide (ITO) or Fluorine-doped tin oxide (FTO) is used as substrate for the photoanode. These materials are commercially available. ITO can be also commercially obtained on a transparent plastic substrate made of polyethylene terephthalate (PET) [72] or other synthetic polymers. Such plastic electrodes can be adapted to non-planar reactor geometries. They have been mainly used for organic photovoltaic and organic LED applications but they may also be useful for PEC cell applications. Several laboratories use non-transparent metal electrodes, principally titanium. In the case when titania is synthesized by electrochemical etching of titanium foils (see Section 4.1.6), the electrode is naturally made of the titanium foil itself. Generally speaking, where the photoanode is exposed to front-face excitation, the electrode can be a non-transparent metal but when excitation of the photocatalyst is made through the electrode, which is used as reactor window, it is necessary to use a TCO. Some electrode assemblies have also been inspired from fuel cells, where the photocatalyst is deposited on conductive textile, like carbon cloth or carbon paper [14].

4.1.2. Choice of photocatalysts

For reasons already exposed in Section 4.1, nanocrystalline titania is the most commonly used functional material to make a photoanode. However, other oxides and other n-type semiconductors have been studied as well. ZnO is one of them. ZnO absorbs light in the UVA as anatase, and has approximately the same band gap and approximately the same CB and VB levels [73,74] (cf. Fig. 4). Some authors claim that ZnO is a more active photocatalyst than TiO$_2$ [74,75], others that titania is better [76] and still others that they are about equally active [77,78]. This discrepancy simply sug-

gests that the performance of a photocatalyst depends, first of all, on some crucial parameters, for example, methods of preparation, nanoparticle size, crystallinity etc. ZnO is considered to be vulnerable to oxidation (ZnO + 2h$^+$ → Zn^{2+} + 1/2O$_2$) [79,80] but this process is impeded in the presence of a sacrificial agent that consumes holes, as is the case of the PFCs. ZnO was frequently used for making photoanodes in the past [79,81,82] and it was the semiconductor with which the so called "current doubling effect" was originally observed (see Section 7.2). As a matter of fact, ZnO nanostructures are more easy to produce and to maintain than those of TiO$_2$. Nanoparticulate ZnO can be synthesized by electrodeposition [83,84] and thus it is possible to apply on plastic electrodes or even textile electrodes [85]. ZnO nanoparticles can be easily dispersed making stable colloidal dispersions [86,87]. ZnO has been synthesized in many different nanostructures like nanoneedles [88], nanorods [87], nanofibers [89], nanowires [90], etc. and it has an inherent ability to crystallize in various geometries resulting in hierarchical architectures [80]. For all these properties, ZnO has been broadly studied, being second studied oxide semiconductor after titania. In conclusion, we might say that ZnO will be a good choice for applying on a photoanode in cases when titania could not be used.

Another interesting oxide semiconductor is Fe$_2$O$_3$. This material has a great advantage, that is, it absorbs visible light (E_g = 2.2 eV [74], cf. Fig. 4) but it is charged with a few disadvantages: it is not very stable in harsh chemical environments and it has very small hole diffusion length (2–4 nm [16]). For this reason, it is necessary to apply Fe$_2$O$_3$ in the form of very thin films [16,91]. The necessity for very thin films was realized also in earlier publications [10,92]. Techniques of spray pyrolysis [10,16,92] have been used for this purpose; however, in a recent publication [91], a colloidal-solution-based process was also successfully employed. Thin films decrease the active cross-section and make the material more chemically vulnerable. For this reason, co-application of other photocatalytic or electrocatalytic materials might be necessary [92]. In any case, Fe$_2$O$_3$ remains an interesting material to study for application in PFCs.

Many other oxide semiconductors have also been studied to mainly examine their photocatalytic degradation capacity. A brief review has been presented in Ref. [74]. Besides TiO$_2$ and ZnO, only SrTiO$_3$ has the energy levels necessary to create active radical species that could efficiently carry out photodegradation process. The importance of this assertion can be understood by the diagram of Fig. 4. This diagram was adapted to data presented in Refs. [74,93–96]. It gives values of the Energy gap E_g and of the position of the conduction band and the valence band levels at pH 7 vs. normal hydrogen electrode (NHE). On the same diagram one sees the redox levels of hydrogen ion reduction (H$^+$/H$_2$), superoxide formation (O$_2$/O$_2^{\bullet-}$), O$_2$ reduction (O$_2$/H$_2$O) and hydroxyl radical formation (OH$^\bullet$/OH$^-$). H$^+$/H$_2$ level in Fig. 4 is given a negative value, since pH 7, according to Eq. (1). The difference between H$^+$/H$_2$ and O$_2$/H$_2$O is about 1.23 V. It must be stressed that the values in the diagram of Fig. 4 are not precise but the diagram is used for explaining the approximate behavior of the depicted semiconductors. First of all, the oxidative power of each photocatalyst is judged by its ability to oxidize OH$^-$ ions to produce highly reactive OH$^\bullet$ radicals. Most of the common oxides have this property, as seen in Fig. 4, i.e. they have a VB, which is more electropositive than the OH$^\bullet$/OH$^-$ level. Fe$_2$O$_3$ is an exception and for this reason Fe$_2$O$_3$ is a poor photocatalyst [74]. A good photocatalyst should also be capable of donating electrons to form the also highly reactive superoxide O$_2^{\bullet-}$ radical species, when the system runs in the presence of oxygen. This is judged by the height of the CB level compared with the O$_2$/O$_2^{\bullet-}$ redox level. This criterion distinguishes TiO$_2$, ZnO and SrTiO$_3$ from other oxides, as already said [74]. The non-oxide semiconductors of Fig. 4 will be discussed in the following section. As a conclusion
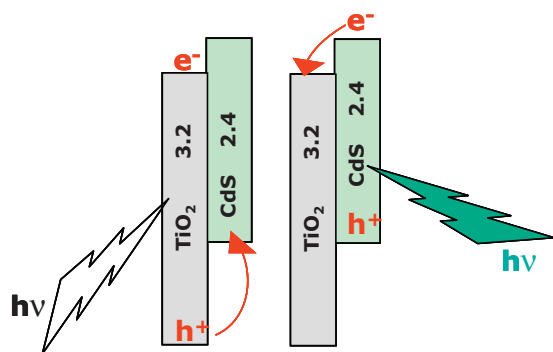
Fig. 5. Illustration of the electron–hole separation in coupled TiO_2:CdS semiconductors by light absorption either in the UVA (left) or in the Visible (right). The majority semiconductor is TiO_2. Under UVA radiation, titania is mostly excited, since it is the majority semiconductor, and the photogenerated hole is injected into the CdS VB. Under Visible radiation, only CdS can be excited and the photogenerated electron is injected in the CB of titania.

to this section, we might say that high E_g oxide semiconductors, in particular TiO_2 and ZnO, which are easy to synthesize and deposit as thin films, are the incontestable champions to employ in PEC cells. However, other oxide semiconductors are not and should not be excluded but should be further studied.

4.1.3. Non-oxide chalcogenides

Non-oxide chalcogenide n-type semiconductors like ZnS,CdS, CdSe, etc. have been extensively studied for application in photocatalytic [97–117] and photoelectrochemical [111,118–137] production of hydrogen. The reason is that they absorb visible light, with the exception of ZnS. However, these substances are vulnerable to oxidation (for example, $CdS + 2h^+ \rightarrow Cd^{2+} + S$), which dissolves the material and destroys it. In the presence of a sacrificial agent, it is possible to harvest holes and impede semiconductor dissolution. Also these materials can be synthesized in the form of core-shell nanostructures [114,116,138–142], which have greater stability. These competing factors fed a lot of research on these semiconductors, both in the past [97–109,118–127] and in recent years [110–117,128–142]. In spite of its high E_g, ZnS has been a popular target of research and this is for the following reasons. The CB and VB levels of this semiconductor are favorably placed, as can be seen in Fig. 4, so that it possesses strong oxidant and reductant power. It combines with CdS so that, by changing proportions, E_g can be tuned within a wide range [105–107,143]. Combination of two semiconductors assists electron–hole separation anyway (see Section 4.1.5). ZnS has also been used to make core-shell nanostructures [141]. A review of the publications related with both photocatalytic and photoelectrochemical production of hydrogen reveals that chalcogenide non-oxide semiconductors have been mainly used with sulfur-containing sacrificial agents like S^{2-}, SO_3^{2-} (see for example, [98,101–103,108,109,111–113,128–131,135]). Much fewer are the cases when other materials, for example, alcohol has been used as a sacrificial agent [136,137]. There are two good reasons to use S^{2-} and SO_3^{2-} ions: these materials are abundant in industrial wastes, therefore, photocatalytic degradation of wastes with simultaneous hydrogen formation is a highly important application; and the presence of these ions repairs any semiconductor loss, since it refills oxidized sulfur. Non-oxide short-band-gap semiconductors are recently very frequently used in combination with wide-band-gap oxide semiconductors, like titania [131–137] (see also Section 4.1.5). Their role in that case is double. They act as titania sensitizers in the Visible at the same time preventing electron–hole recombination, since electron is transferred to a separate nanoparticle. This property is depicted in Fig. 5. In conclusion, we might say that non-oxide metal sulfide semiconductors are

very interesting systems to study for application in PEC cells. They are mainly used with S^{2-} and SO_3^{2-} sacrificial agents but other substances are not excluded. They can be used as sensitizers of wide-band-gap oxide semiconductors while in combination with the wide-band-gap ZnS, they yield binary semiconductors with a broad band-gap tuning.

4.1.4. Doping of titania for Visible absorption

Among all studied semiconductor photocatalysts, titania remains the most popular of all, for the already explained reasons. The number of publications that treat titania photocatalyst is huge and is still increasing. After all this work, there are still open questions that feed research on titania. These questions will be briefly reviewed in the following sections including the present one, by focusing on titania applications to PEC cells.

In order to make it absorb in the Visible, titania has been doped by either metal (cation) or non-metal (anion) dopants. Metal dopants substitute titanium in the crystal lattice while non-metal dopants substitute oxygen. This substitution creates energy states within titania band gap, which practically make bang gap smaller, thus the new material absorbs visible light. Titania doping has been reported in many papers in the past including several review papers. We cite only a few of the very recent reviews [144–149]. The general impression that one obtains from recent reviews is that there exists a lot of skepticism about the efficiency of doped titania. First, it must be made clear that real metal doping should be distinguished from oxide catalyst mixtures. Substitution of titania in the lattice is not easy. Heating at very high temperature leads to doping [23] but this also leads to extensive decrease of the catalyst active surface. In general, the presence of the dopant creates an impurity that becomes a recombination site [145,149] with catastrophic results on photocatalysis. Therefore, it is practically better to use well-formed active titania excited in the UV than doped titania, even if it absorbs visible light [150]. Absorbance in the Visible is usually low any way [151] compared with absorbance in the UVA. Some researchers have doped titania with ion implanting techniques [152] and they did create Visible responsive titania. However, this technique is not useful for massive catalyst production.

Non-metal doping (for example, N,C,S, etc.) can be obtained at lower temperature and it is generally easier. This has created a rich literature but skepticism still exists [151,153–156], at least, as far as applications to PEC cells is concerned. Non-metal doping of titania makes materials with interesting photophysical properties [149,157,158] and this leaves a lot of ground for further research. In conclusion, doping of titania with metals or non-metals for absorption in the Visible, for the time being, has not created more efficient PEC cells, but this question is open and further research is worth.

4.1.5. Titania in combined-catalyst systems

When titania is mixed with a co-catalyst, the photocatalytic capacity of the mixture usually increases. In order to understand the behavior of such catalyst mixtures, it is necessary to separately study a few characteristic cases.

Combination of nanocrystalline titania with noble metal nanoparticles has made very successful combined catalysts. As depicted in Fig. 1A, showing a metal nanoparticle in contact with a semiconductor nanoparticle, the metal scavenges photogenerated electrons, thus facilitating electron–hole dissociation and facilitating reductive interactions. In that case, the metal acts as electrocatalyst in intimate contact with the photocatalyst. Electron–hole dissociation is the key factor that makes the role of titania successful or not [47–50,54–59]. The best metal electrocatalyst is Pt, followed by Pd and Au. By first look, this could be explained by the fact that Pt has the highest work function; therefore, it makes the best electron sink for the photogenerated electrons. But there
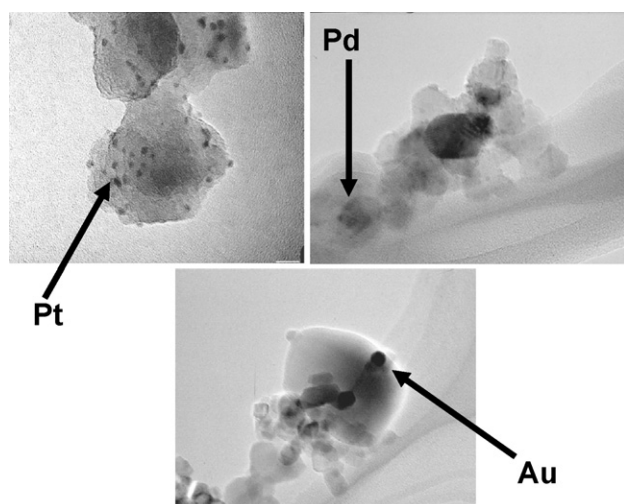
Fig. 6. TEM images of Pt, Pd and Au nanoparticles deposited on titania nanoparticles. The size of Pt nanoparticles ranges within 2–3 nm, of Pd 3–5 nm and of Au 10–20 nm (Adapted from Ref. [57]).

is more to the role of Pt. Pt makes the smallest metal nanoparticles and the finest distribution on host nanoparticles [57,159] (cf. Fig. 6) and this is considered to play an important role in electron–hole dissociation. Indeed, in simple physics, it is more probable to find electrons in two separate particles than in the same particle, since they will then repel each other. Therefore, it is easier to scavenge electrons by a more fine and more numerous distribution of metal nanoparticles.

Nanocrystalline titania as well as nanocrystalline ZnO can be combined with another oxide catalyst. Several such cases have been studied and the related literature is very rich [20,160–172]. Combinations between oxide semiconductors are expected to assist electron–hole separation. Take, for example, the case of TiO_2 and SnO_2. Their energy levels are given in Fig. 4. Photogenerated electrons in titania may be transferred to the lower lying conduction band of SnO_2 (in analogy to CdS in Fig. 5) thus leading to electron–hole separation and to higher efficiency of the photocatalytic process. Such combinations can be devised with several coupled semiconductors: TiO_2:SnO_2 [160,163,164]; TiO_2:WO_3 [162]; TiO_2:RuO_2 [170]; TiO_2:V_2O_5 [172]; ZnO:SnO_2 [167]; etc. Of particular interest are the so called industrial coupled catalysts like TiO_2:V_2O_5 [173]. When the minority catalyst (i.e. V_2O_5) comes in small quantities then it is possible to treat TiO_2:V_2O_5 as all the other

coupled photocatalysts. It is even reported that since the minority catalyst absorbs visible light, the photocatalytic function extents in the Visible [172]. However, the major function of V_2O_5 in industrial catalysts is a redox mechanism, in which the target hydrocarbon reduces the catalyst and the catalyst is re-oxidized by the oxygen in the feed [173]. In the case of photocatalysis, the excitation of titania can lead to *V* reduction and this provides an additional mechanism of electron retention and electron–hole dissociation. The same mechanism may also be valid in the case of the TiO_2:RuO_2 couple or other similar situations. It is then suggested that coupled photocatalysts should be distinguished in those, which induce simple electron injection and those working by a redox mechanism.

A third distinguished category of combined catalysts is the combination of titania (or ZnO) with non-oxide semiconductors [131–137,139,142], for example TiO_2:CdS (see also Section 4.1.3). The minority photocatalyst is again the non-oxide semiconductor. In the presence of a sacrificial agent that retains holes and impedes S^{2-} oxidation, the function of CdS in the TiO_2:CdS combination is among the purest cases of charge injection, as illustrated in Fig. 5. When the excitation is made by UV light, the majority photocatalyst absorbs most photons. Photogenerated holes then jump onto the less positive VB of CdS while only part of them oxidize OH^- ions. When excitation is made by visible light, CdS absorbs photons, is excited and injects excited electron onto the CB of titania. Experimental data obtained by the present author using TiO_2 modified by loading with CdS quantum dots (QDs) [17,136] revealed that the current increased in the presence of CdS by both UVA and Visible excitation. This current increase demonstrates the efficiency of electron–hole separation by the combined catalyst. Loading of titania with, for example, CdS or ZnS QDs is very easy. It can be done by Sequential Ion Adsorption from solutions of Cd^{2+} or Zn^{2+} and S^{2-} [136,137,174]. This is another advantage of using non-oxide QDs, since deposition is done under ambient conditions.

Is it in the interest of PEC cells and, in particular, to PFCs to employ combined catalysts? The answer to this question must take into account the following opposing trends. The highest currents are obtained in situations when all photogenerated electrons are channelled through the external circuit towards the cathode. This means that no electrons are retained by the minority catalyst or by oxygen present in the electrolyte around the anode compartment. However, in that case, the oxidative power of the photoanode is limited and the photodecomposition of the organic substance is incomplete. It may then be necessary to partly retain photogenerated electrons so as to make sure that photodecomposition goes on as expected. In a few words, a PEC cell should ideally work under a delicate balance between current flow and photodegradation. This
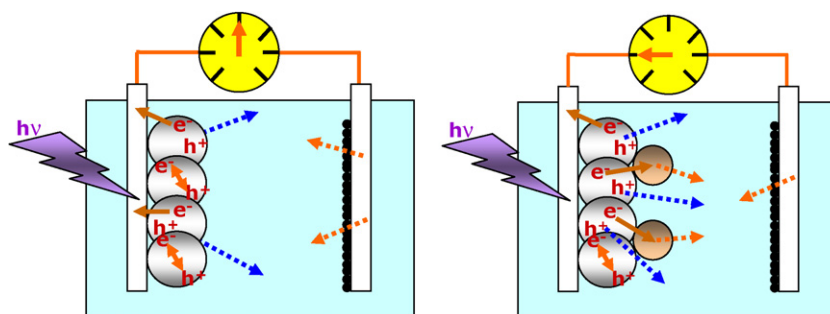
Fig. 7. Illustration of the function of the cell with single catalyst photoanode (left) and coupled catalyst photoanode (right). The larger circle corresponds to the majority catalyst (for example, TiO_2) and the smaller circle to the minority catalyst (for example, another semiconductor or Pt). In the first case, the current is higher but the photodegradation possibilities are limited. In the second case, the current is smaller but the photodegradation possibilities are higher. In other words, in the single catalyst case (left), the number of charge carriers that can participate in oxidative interactions can be at maximum equal to the number of electrons flowing through the external circuit. In the case of combined catalysts (right), more holes are available because of the increased number of electron–hole separations while electrons injected into the minority catalyst will be also available for oxidative interactions by formation of superoxide radicals in the presence of oxygen.

situation is illustrated in Fig. 7, which distinguishes between the two cases of pure catalyst and combined catalyst.

4.1.6. One-dimensional titania nanostructures

As it is well known, a great part of the recent research on nanostructured titania is devoted to the synthesis of one-dimensional nanostructures, like nanorods, nanotubes, nanowires, etc. These nanostructures are expected to assist photogenerated charge carrier conduction and electron–hole separation and also increase the photocatalyst active surface. The following lines briefly review some related characteristic works.

Titania nanotubes can be electrochemically etched on a titanium foil. Typical examples can be found in Refs. [12,175–178]. A titanium foil is anodized in the presence of a corrosive electrolyte producing well-formed and well-alligned titania nanotubes after heating at high temperature. The pore diameter and the wall thickness of the nanotubes vary with the applied voltage and the duration of anodization. Details on the experimental procedure can be found in the above works. Typical thickness (length) of the nanotube array ranges from about 0.5 μm [178] to 20 μm [179]. The titanium foil with the TiO_2 nanotube pattern can be used as photoanode in a PEC cell [12,177–179]. During the process of annealing, non-metal doping of the nanotubes can be obtained in the presence of appropriate reagents, which could then give a PEC response in the Visible [12,177,178]. In a review paper recently published by the C.A. Grimes group [179] various aspects of Ti anodization for application in photoanodes have been presented. For example, improvement of light absorption cross-section was observed by using non-planar Ti electrodes, like Ti pipes. This particular subject of research is without doubt interesting and it is evolving.

Titania nanotubes can be also obtained by hydrothermal treatment of titania powder for several hours in an autoclave, at high pH, followed by mild acid washing [180–182]. This method produces nanotubes that look like hollow nanowires [182] rather than the aligned species obtained by anodization. Nanowires can be also made by treating metallic titanium [183] or titania film [184]. These structures have been mainly used in hybrid solar cells or dye-sensitized solar cells but some applications in water splitting have also been reported [184]. The principal technique to make long nanowires is by electrospinning [185]. Electrospinning is a simple method [185–187] but necessitates a careful choice of precursor materials. Experimental details can be found in the above papers.

In conclusion, the number of works published on titania nanostructures is large. Among these works, titania synthesized by anodizing metallic titanium seems to be the most so far applied material for photoanodes in PEC cells but the rest of the nanostructures are not excluded.

4.1.7. Combination of titania with carbon nanostructures

We are living in a world of "nano-mania". It seems that there exists no nanostructure which has or will not sooner or later be studied by some research group for PV or PEC application. Not all combinations are worth trying but the ardour, which these materials are studied with, always carries promise that will find its valued application. In this section, a very brief review of titania–carbon mixtures will be reported.

Several authors have recently studied combinations of nanocrystalline titania with carbon nanostructures, mostly Multi-Wall Carbon NanoTubes [188–193] or, less frequently, Single-Wall Carbon NanoTubes [194]. The presence of these materials is expected to assist electron conduction and thus electron–hole dissociation. All authors report improvement of efficiency in all their applications. However, the author of this paper believes that all these sophisticated materials necessitate a careful preparation procedure that sometimes is not worth the effort. Only the "good" results are reported and usually no mention is made on stabil-

ity. As with all other materials so far discussed, comparisons are difficult to make because efficiency dramatically depends on methods of preparation, particle size, conditions of measurement, etc. In addition, in mixtures with carbon, there is always the question of allowing enough light to reach the semiconductor. All these questions are expected to feed a lot of research on these materials and no version of them is considered completed.

4.2. Cathode

Large volumes will be necessary to record all works dealing with the various semiconductors used to make photoanodes. On the contrary, the choice for cathode electrodes is very limited. Many researchers have used a Pt wire or a Pt foil as counter electrode, while a better choice is platinized Pt foil or platinized stainless steel mesh [61,62]. Platinization can be made by some different methods. One such method is electrolytic reduction in a solution containing H_2PtCl_6 and appropriate electrolytes [6] or the corresponding salt K_2PtCl_6 [61,62]. However, in most cases it is preferable to cover platinum with Pt-Black [13]. Pt-Black is a fine powder of platinum and it is called this way because of its black color. By depositing Pt-Black on a Pt foil, the functional area of the electrode becomes much larger than its geometrical area. Pt-Black can be cast, sprayed or hot-pressed on the electrode.

Usually annealing at high temperature is necessary in order to permanently attach Pt-Black on the electrode. An even better choice is to use the so-called gas-diffusion-electrodes inspired from fuel cells, which are made of carbon cloth or carbon paper. In that case, Pt-Black is mixed with Carbon-Black, i.e. carbon fine powder. A detailed description of the fabrication of such electrodes can be found in Refs. [17,71].

An efficient cathode reflects on the charge-transfer resistance R_{ct} at the electrode/electrolyte interface and R_{ct}, in turn, reflects on the value of the fill factor (FF) of the cell. FF also depends on the quality of other parts of the cell but by keeping all other parameters the same, one can compare one cathode electrode from another by the value of the FF. More on FF are found in Fig. 8 and its caption. Pt is the best electrocatalyst but it does have some disadvantages. In addition to the fact that it is very expensive, it may be oxidized and it migrates on the electrode, forming large agglomerates that eventually lead to electrode deterioration. Therefore, there is a large effort to find alternative solutions. Most of the works dealing with this matter belong to the field of electrocatalysis related with fuel cells [195] including microbial-fuel-cells [196,197]. Furthermore, there is also an important activity related with counter electrodes for dye-sensitized solar cells [198–200].

4.3. Electrolyte

A review of the literature on PEC cells shows that the choice of electrolytes is also limited. With titania on the photoanode electrode, the most frequently used electrolyte is NaOH or KOH [12,15,17,60,71,155,177,184,187]. The reason is to obtain high pH. At 1 M NaOH, the pH is close to 13.0. Thus in the presence of high OH^- concentration, efficient hole scavenging and production of hydroxyl radicals is ensured. This is particularly important when an organic sacrificial agent is added, which is expected to be photodegraded during PEC cell operation [17,71,187]. When the cell is structured in two compartments, a basic electrolyte is frequently introduced in the anode compartment and an acidic electrolyte (H_2SO_4) in the cathode compartment thus offering chemical bias to the cell [15,60,136,184,201], according to Eq. (1). In addition to chemical bias, the acidic electrolyte in the cathode compartment facilitates hydrogen ion mobility. If the membrane separating the two compartments is a proton-transfer membrane, then the acid sustains its functionality. However, as already said,
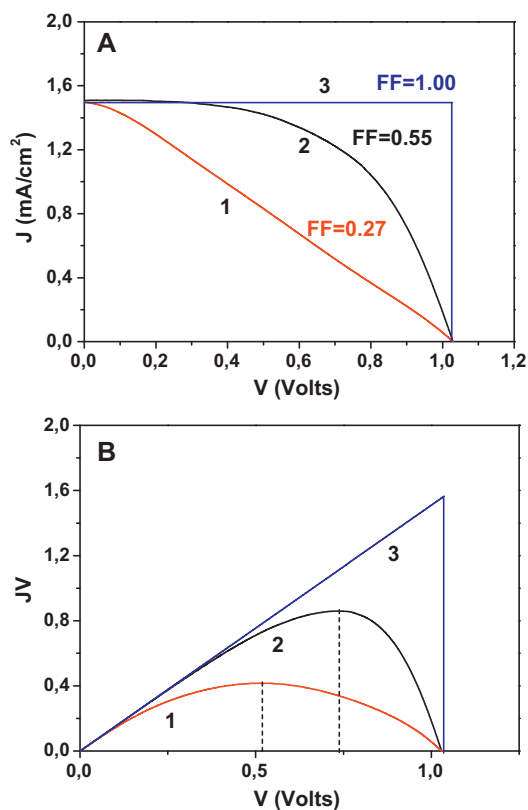
Fig. 9. Photograph of a convenient laboratory PEC H-shaped reactor made of pyrex glass. Ion-transport membrane is supported in the middle. Fittings with tubing allow electrode connections and gas inlet–outlet.

gen ions and the functionality of the Nafion membrane while in Refs. [3] and [148] an acidic electrolyte was used for reasons of system study. Finally, Na_2S and Na_2SO_3 electrolytes have systematically been used with non-oxide semiconductors, like CdS and ZnS [128,131–134], since these substances contain sulfur that can be oxidized ($2S^{2-} \rightarrow S_2^{2-}$ and $S^{4+} \rightarrow S^{6+}$) and thus act as sacrificial agents that sustain the integrity of these semiconductors. Titania loaded with CdS QDs has been employed with NaOH as electrolyte in the presence of organic sacrificial agents but the stability of this combination has not been tested [136,137].

5. PEC cell design

By PEC cell design, we mean the actual geometry employed to make a laboratory prototype photoelectrochemical cell. Many cells have the geometry depicted in Fig. 2. It is a typical case of an H-shaped cell. It is structured in two compartments separated by an ion-transport membrane. One such cell with compartments of cylindrical geometry, carrying appropriate fittings for electrical connections and gas inlet–outlet can be seen in the photograph of Fig. 9. In this cell, each compartment can accept about 200 ml of electrolyte, which can be easily treated by gas bubbling or magnetic stirring. Bubbling is not easy in small volumes, where a recirculation of the electrolyte is necessary and this creates some practical difficulties. However, in the cell of Fig. 9, the distance between the anode and the cathode electrode is 17 cm. This is rather too large a distance that increases the ionic resistance of the cell. The distance between anode and cathode affects the fill factor of the cell (cf. Fig. 8), that is, FF decreases as the distance (and the ionic resistance) increases. It is then preferable to bring the two electrodes as close as possible. Thus in Ref. [14], where a fuel cell running in reverse is presented, a membrane-electrode assembly has been constructed where an electrode bearing titania and an electrode bearing electrocatalyst sandwich a Nafion membrane. Therefore, the distance between the two electrodes is minimal. In Refs. [61,62], the electrocatalyst is deposited on a steel mesh electrode, which is placed very close to the anode. The system of the two electrodes is submerged in the electrolyte thus making a one-compartment cell. Finally, in Ref. [17], half a membrane-electrode assembly has been constructed with a carbon cloth loaded with Pt/CarbonBlack electrocatalyst attached on a Nafion membrane. Titania was on a separate FTO electrode. We believe that cell geometry leaves a lot of space for inspiration but the above examples give a good starting guide.

Fig. 8. Fill factor. The quality of a device that converts solar energy to electricity can be characterized by its fill factor (FF). The output voltage of the device depends on the resistance of the external load through which the current flows. The larger the resistance the larger the voltage. When the resistance is infinite, i.e. very large, the voltage is equal to the open-circuit voltage V_{oc}. When the resistance is zero, then the voltage is also zero and the current obtains its maximum value, equal to the short-circuit current I_{sc}. The current is usually expressed as current density J, i.e. the quotient of the current divided by the geometrical surface of the electrodes. If J is the current density delivered by the device at voltage V, the electric power density is given by the product JV. FF is then given by the following equation:

$$FF = \frac{(JV)_{max}}{J_{sc}V_{oc}}. \qquad (2)$$

where $(JV)_{max}$ is the maximum value of the power density. The present figure explains the meaning of FF to better understand it. In part (A), there are three plots. Curves 1 and 2 describe two real situations and the perpendicular lines (3) correspond to an ideal situation. The ideal "curve" 3 represents a situation where, no matter how large the external load is, the device outputs always the same (maximum) current. However, in real situations, when the resistance of the external load increases, which means that the output voltage increases, the current decreases. The variation of the output electric power density vs. voltage is given by the corresponding curves in part (B). The latter always have a maximum but this maximum is smaller, less sharp and is displaced to smaller voltages as the device departs away from the ideal case. The value then of the FF and the position and the value of $(JV)_{max}$ is indicative of the quality of the device. In the case of PEC cells, large ionic resistance, large charge-transfer resistance at the electrode/electrolyte interface and other factors may unfavorably affect the FF.

chemical bias is not suggested for a self-sustained cell. High pH electrolyte has also been used with Fe_2O_3 photoanodes [10,16]; however, other oxides, like ZnO, cannot sustain this harsh chemical environment and necessitate milder electrolytes like KNO_3, Na_2SO_4 or $LiClO_4$ [79,81,157,178]. Since the presence of OH^- helps photodegradation procedure, some authors add NaOH at moderate concentrations (0.1 M) [81,155]. Na_2SO_4 has been used as electrolyte in Bio-photofuel cells where the photodegradable substances are of biological origin [13,61,64]. Oxide semiconductor photoanodes have less frequently been used with acidic electrolytes [3,14,148]. In Ref. [14], the PEC cell was a fuel cell running in reverse and acid was necessary to sustain the availability of hydro-

6. Photodegradable organic and inorganic wastes

6.1. Choice of photodegradable substances

One of the advantages of the photocatalysts, especially, the oxide semiconductor photocatalysts, is that they are not selective. Any organic substance is a potential target for photodegradation. This advantage is carried over to photoanodes and eventually to PFCs (Photofuelcells). In this sense, a PFC is more interesting than a fuel cell. In a fuel cell, costly catalysts are necessary to decompose a few selected organic fuels and it is frequently necessary to carry out the process at elevated temperature. In the case of a PFC, the exciting radiation is the only necessity. The process is realized at ambient conditions without selectivity with respect to the fuel, i.e. the photodegradable organic substance. Furthermore, water itself can be split in a PEC cell and produce a fuel. This is a good point to start but not all organic substances offer the same energy output, either in terms of electric power generation or in terms of molecular hydrogen production. Most researchers choose to study methanol, ethanol or glycerol as model fuel [14,17,47,48,50,54–59,65,71,81,136,137,164,187,201]. There are three good reasons for this choice: (1) these substances give the highest yield; (2) they have been extensively studied, so there exists a lot of information about them; and (3) they are products of biomass, therefore, available and renewable. In particular, glycerol is a byproduct of bio-diesel [202] and it is now available in large quantities so that it can be treated as a waste material. In addition to small-chain-length alcohols and glycerol, other polyols, sugars, organic acids, aldehydes and ketones have also been a popular choice for PC and PEC production of hydrogen [21,37,52,53,56,65,165,166,201]. The overall reaction scheme for photocatalytic reforming, i.e. photodecomposition and mineralization in the absence of O_2 with water playing the role of the oxidant, for substances of the general formula $C_xH_yO_z$, is given by the following reaction [203]:

$$C_xH_yO_z + (2x - z)H_2O \rightarrow xCO_2 + (2x - z + (y/2))H_2 \quad (III)$$
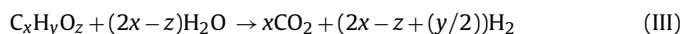
When this scheme is put into effect in a PEC cell, a relatively large number of electrons should be conducted through the external circuit to reduce hydrogen ions and produce molecular hydrogen. For example, in the case of alcohols it corresponds to 6 electrons per carbon atom. However, reaction (III) is an overall scheme and it is realized in steps (see next section). Smaller size alcohols are in fact easier to photodegrade and to mineralize than larger molecular weight homologues.

Recent works have shown that a broad choice of organic substances that are considered waste materials or pollutants can be photodegraded to produce electricity [13,61–64,171,201]. Particular reference must be made to the works of Kaneko et al. [13,61–64], who have treated a large variety of biological wastes to run a PFC. A typical model fuel in these works was ammonia obeying the following mineralization scheme:

$$2NH_3 \rightarrow N_2 + 3H_2 \quad (IV)$$

while similar routes can be traced for more complicated substances. All these examples show that there exists a good basis to support the idea of employing PFCs to decompose organic wastes and produce usable forms of energy, like electricity and hydrogen.

In the case of non-oxide semiconductors, the sacrificial agent is rarely an organic material [136,137]. In most cases, inorganic materials has been used, as already explained in Section 4.3, that is, almost exclusively Na_2S and Na_2SO_3. However, PEC cells running with QDs attached on titania do work with organic materials like ethanol and glycerol. Further research on such systems should be conducted.
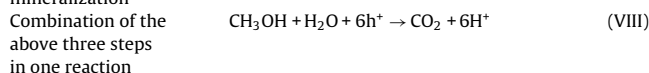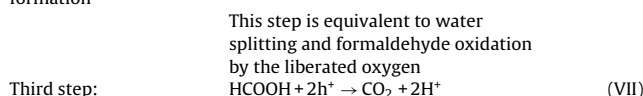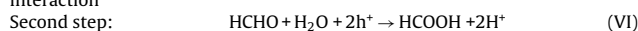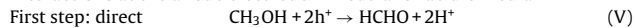
6.2. Photodegradation routes and intermediates

Photodegradation and mineralization routes have been studied for the most popular target organics like methanol, ethanol and glycerol. Here we record these reaction schemes separately for each substance, having in mind their possible application to PEC cells.
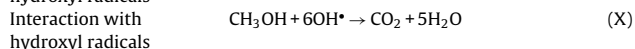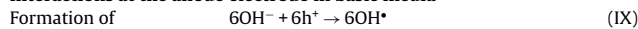
When the semiconductor photoanode is excited by absorption of photons, electron–hole pairs are generated. Holes drive the oxidation reactions; therefore, the following interactions should take place at the anode electrode (adapted according to Refs. [31,47,54,71,81,136,203,204,205]):

Methanol

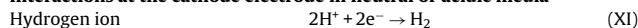**Interactions at the anode electrode in neutral or acidic media**

First step: direct methanol–hole interaction	$CH_3OH + 2h^+ \rightarrow HCHO + 2H^+$	(V)
Second step: formic acid formation	$HCHO + H_2O + 2h^+ \rightarrow HCOOH + 2H^+$	(VI)
	This step is equivalent to water splitting and formaldehyde oxidation by the liberated oxygen	
Third step: mineralization	$HCOOH + 2h^+ \rightarrow CO_2 + 2H^+$	(VII)
Combination of the above three steps in one reaction	$CH_3OH + H_2O + 6h^+ \rightarrow CO_2 + 6H^+$	(VIII)

Interactions at the anode electrode in basic media

Formation of hydroxyl radicals	$6OH^- + 6h^+ \rightarrow 6OH^\bullet$	(IX)
Interaction with hydroxyl radicals	$CH_3OH + 6OH^\bullet \rightarrow CO_2 + 5H_2O$	(X)

The distinction of interactions in those occurring in neutral or acidic media from those taking place in basic media has the following meaning. When the number of hydroxyl ions is limited or is very small, it is expected that methanol and its intermediates, i.e. formaldehyde and formic acid, will directly interact with holes and will induce the reactions (V)–(VIII). However in basic media, where the number of OH^- is large, it is expected that interactions will most probably follow the scheme of (IX) and (X), since OH^- are very efficient hole scavengers. It is also possible that other routes, not described by the above reactions, might be in effect, however, not disturbing the mineralization process. For example, oxidation of formaldehyde might be effectuated by direct interaction with holes than through water splitting, since formaldehyde is much stronger electron donor than water.

The photogenerated electrons drive reduction interactions either in situ, as shown in the PC operation of Fig. 1A or at the cathode electrode during PEC operation. In the presence of oxygen, hydrogen ions are consumed but in the absence of oxygen, molecular hydrogen is produced. The corresponding interactions are the following:

Interactions at the cathode electrode in neutral or acidic media

Hydrogen ion reduction in the absence of oxygen	$2H^+ + 2e^- \rightarrow H_2$	(XI)
Oxygen reduction in the presence of oxygen	Reactions (I) and (II), already given in Section 3	

Interactions at the cathode electrode in basic media

Water reduction in the absence of oxygen	$2H_2O + 2e^- \rightarrow 2OH^- + H_2$	(XII)
Water reduction in the presence of oxygen	$H_2O + 1/2O_2 + 2e^- \rightarrow 2OH^-$	(XIII)
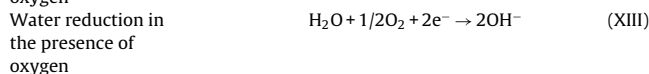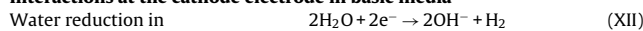
As in the case of the anode, we distinguish behavior under neutral or acidic conditions and under basic conditions. Combination of reaction (XI) with reaction (VIII) produces the complete methanol reforming reaction

$$CH_3OH + H_2O \rightarrow CO_2 + 3H_2 \tag{XIV}$$

which is an extract of reaction (III) and it is realized in the absence of oxygen. In that case, as already said, water plays the role of the oxidant by means of reaction (VI). In basic environments, we note that OH^- is consumed during reactions (IX) and (X) but it is reproduced during either reaction (XII) or (XIII). Oxygen reduction reactions (I) and (II) 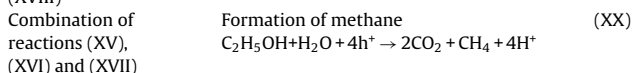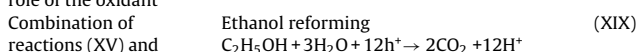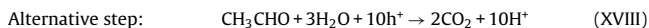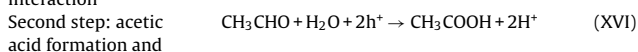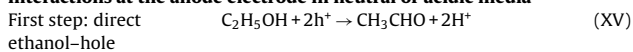in the presence of O_2 can lead to hydrogen peroxide or to water formation. In principle, H_2O_2 is favored in most cases [31] since it is formed at lower potential. In conclusion, when methanol is photodegraded in a PEC cell, molecular hydrogen can be produced at the cathode electrode in the absence of oxygen, both at low and at high pH. Electrons flow in the external circuit and their number is exactly related with the number of reduced species.
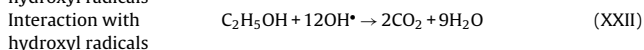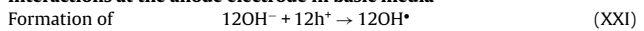
The corresponding interactions in the case of ethanol are given by the following reactions (adapted according to Refs. [48,50,57,71]):

Ethanol

**Interactions at the anode electrode in neutral or acidic media**

First step: direct ethanol–hole interaction	$C_2H_5OH + 2h^+ \rightarrow CH_3CHO + 2H^+$	(XV)
Second step: acetic acid formation and mineralization by methane evolution	$CH_3CHO + H_2O + 2h^+ \rightarrow CH_3COOH + 2H^+$	(XVI)
	$CH_3COOH \rightarrow CH_4 + CO_2$	(XVII)
Alternative step: mineralization of acetaldehyde with water playing the role of the oxidant	$CH_3CHO + 3H_2O + 10h^+ \rightarrow 2CO_2 + 10H^+$	(XVIII)
Combination of reactions (XV) and (XVIII)	Ethanol reforming $C_2H_5OH + 3H_2O + 12h^+ \rightarrow 2CO_2 + 12H^+$	(XIX)
Combination of reactions (XV), (XVI) and (XVII)	Formation of methane $C_2H_5OH + H_2O + 4h^+ \rightarrow 2CO_2 + CH_4 + 4H^+$	(XX)

Interactions at the anode electrode in basic media

Formation of hydroxyl radicals	$12OH^- + 12h^+ \rightarrow 12OH^\bullet$	(XXI)
Interaction with hydroxyl radicals	$C_2H_5OH + 12OH^\bullet \rightarrow 2CO_2 + 9H_2O$	(XXII)

As for methanol, different reaction schemes are presented for neutral or acidic pH and for basic pH. There are many similarities of the above reactions with those referring to methanol but there also some differences. Acetaldehyde can go through two alternative routes, one of them leading to acetic acid formation, limiting hydrogen but favoring methane production. Methane production [48,50,52,206,207] as well as other possibilities for acetic acid decomposition (reaction (XX)) and, more generally, acetaldehyde decomposition [31,208,209] has been reported in several publications. Ethanol reforming reaction proceeds by means of interactions, where water plays the role of the principal oxidant [48] but this role is degraded in the case of methane formation. It is then expected that reaction (XX) will be mostly favored in the presence of oxygen [207].

Reactions (XI)–(XIII) are not specific to methanol and apply to any sacrificial photodegradable substance. Obviously, they also apply to ethanol. Combination of reaction (XI) with reaction (XIX)

produces the complete ethanol reforming reaction [58],

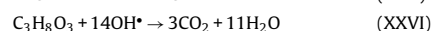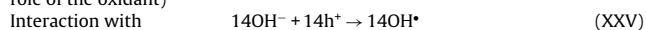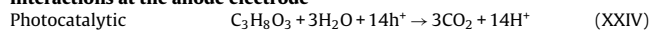$$C_2H_5OH + 3H_2O \rightarrow 2CO_2 + 6H_2 \tag{XXIII}$$
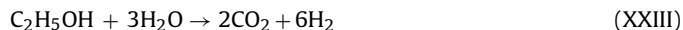
which is an extract of reaction (III) and it is realized in the absence of oxygen. For the rest, everything applies as in the case of methanol.

For longer chain-length alcohols, it is expected that the photodegradation route will be similar with those of methanol and ethanol. Intermediate steps may follow alternative possibilities, as in the case of ethanol. Reforming of each alcohol in the absence of oxygen will obey the general reaction scheme given by reaction (III) [203]. The same applies not only to alcohols but also to polyols, sugars, organic acids, etc. [56], verifying the rule of reaction (III). One such case is glycerol, as already said. Papers that report mechanistic studies in the case of glycerol are less frequent than for lower alcohols. Photodegradation steps of glycerol leading to mineralization are given in Ref. [55]. Hydrogen production by photocatalytic degradation of glycerol in the absence of O_2 was studied in Ref. [59] and was indeed found to follow the scheme of reaction (III). The following reactions summarize the behavior of glycerol.

Glycerol

Interactions at the anode electrode

| Photocatalytic reforming of glycerol in neutral or acidic media in the absence of O_2 (water plays the role of the oxidant)	$C_3H_8O_3 + 3H_2O + 14h^+ \rightarrow 3CO_2 + 14H^+$	(XXIV)
Interaction with hydroxyl radicals in basic media	$14OH^- + 14h^+ \rightarrow 14OH^\bullet$	(XXV)
	$C_3H_8O_3 + 14OH^\bullet \rightarrow 3CO_2 + 11H_2O$	(XXVI)

Such general reaction schemes have been obtained also for other organic materials, like azo-dyes [43]. For the interactions at the cathode, as already said, reactions (XI)–(XIII) describe what goes on independently of the employed target organic substance.

Reactions taking place at the anode, for all cases mentioned so far, do not make clear what happens in the presence of oxygen. Oxygen retains an important percentage of the photogenerated electrons producing $O_2^{\bullet-}$ radicals, which lead to faster photodegradation of the target substance. Retaining of electrons means smaller current flowing through the external circuit, therefore, fewer reductive interactions and thus smaller quantity of molecular hydrogen production. From one point of view, it is then preferable to run the anode in the absence of O_2. However, this is not without consequences. Mineralization of the target substance may be impeded under non-aerated conditions [208,209]. Therefore, a PFC should run by achieving a delicate balance between factors favoring electron flow and factors favoring organic waste photocatalytic degradation (cf. discussion in Section 4.1.5 and Fig. 7).

Waste materials of biological origin have been systematically studied by Kaneko and co-workers [61–64]. One such material is ammonia. Interactions at the anode and the cathode are represented by the following reactions [61]:

Ammonia

Anode	$2NH_3 + 6h^+ \rightarrow N_2 + 6H^+$	(XXVII)
Cathode	$3/2O_2 + 6H^+ + 6h^+ \rightarrow 3H_2O$	(XXVIII)
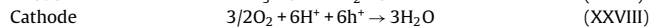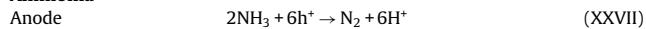
These reactions are carried out in a one-compartment cell in the presence of O_2.

When sulfide semiconductors are used as photocatalysts, almost systematically, the sacrificial agents are inorganic, like Na_2S or Na_2SO_3. In these cases the oxidative reactions at the anode electrode are the following [101,103,109]:

$$SO_3^{2-} + 2OH^- + 2h^+ \rightarrow SO_4^{2-} + H_2O \tag{XXIX}$$

$$2SO_3^{2-} + 2h^+ \rightarrow S_2O_6^{2-} \tag{XXX}$$

$$2S^{2-} + 2h^+ \rightarrow S_2{}^{2-} \tag{XXXI}$$
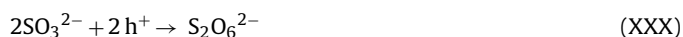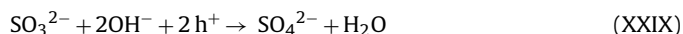
The above reaction schemes do not cover all reported cases but they offer a concrete basis to understand mechanistic studies applying to PEC cells. To finish this section, one more question seeks an answer. Should the pH of the electrolyte be acidic, neutral or basic? If chemical bias is the prime interest, it is obvious that the pH in the cathode compartment should be low and that of the anode compartment high. However, the cell can run without chemical bias under aerated conditions as in Ref. [71], therefore, chemical bias is not always necessary. The question of choosing the right pH has been mainly addressed by studies of PC hydrogen production [50,55,59]. Most researchers agree that a neutral or mildly basic pH gives the best results. More work is necessary, in order to make a clear picture also for PEC cells.

7. Efficiency of PEC cells

7.1. Models calculating PEC cell efficiency

The calculation of the efficiency of PEC cells has raised some problems. The efficiency of a PV device is simply the ratio of the electric power output by the device divided by the light power incident on the device. In the case of PEC cells, measurement of the efficiency is more complicated. The reason is that in addition to the energy of the exciting radiation, one needs to also take into account the effective output energy related to the produced fuel, the chemical energy liberated by the photodegradable substance plus the energy input by any applied bias. Unfortunately, no common language has been so far found that would standardize and simplify these parameters. A recent review lists the different methods of calculating PEC cell efficiency and the various problems faced in applying the related models [210]. In the present paper we make reference to some models of calculating cell efficiency, which are simple and unambiguously represent what they are designed for.

The following two quantum efficiencies are generally defined for solar cells:

(1) External Quantum Efficiency (EQE) and incident photon to current conversion efficiency (IPCE). EQE of a solar cell is the ratio of the number of charge carriers produced by the cell over the number of photons incident on the cell. IPCE is one way to express external quantum efficiency. IPCE is a measure of the effectiveness of the cell to convert the incident photons of a *monochromatic* radiation into electric current [210]. It is given by the following equation:

$$IPCE = \frac{1240 \times J_{sc}(mA/cm^2)}{\lambda(nm) \times P(mW/cm^2)}, \tag{3}$$

where J_{sc} is the short-circuit current density and P the incident radiation intensity at a given wavelength λ. IPCE is a pure number without units. The number 1240 carries the matching units. By recording IPCE at different wavelengths, it is possible to judge the effectiveness of the cell with respect to the spectral response of a photocatalyst or a system of combined photocatalysts or a sensitized catalyst. The value of IPCE is expected to vary between 0 and 1.

(2) Internal Quantum Efficiency (IQE). IQE is the ratio of the number of charge carriers produced by the cell over the actual number of photons absorbed by the cell. Not all incident photons are absorbed by the cell, since a percentage of them passes through the cell or is reflected on the surface. Therefore, IQE is expected to be a larger number than EQE but it also varies between 0 and 1.

Both EQE and IQE can be used to express efficiency of PEC cells. Indeed, IPCE has been measured in several occasions [15,17,62,67,69,71,134,211,212]. In most cases IPCE is expressed as IPCE% by multiplying IPCE of Eq. (3) by 100. Thus IPCE% is expected to vary between 0 and 100. In most cases, IPCE% values for PEC cells are small [62,211,212]. Some authors found relatively large

values because the wavelength band used was not narrow enough [17,71]. Therefore, comparison makes sense only for the same system and by changing only one parameter at a time. Unusually high values of IPCE in PEC cells may also ensue from "current doubling" phenomena (see Section 7.2).

Another expression equivalent to EQE for a PEC cell (represented by η) can be calculated by the following equation [210]:

$$\eta = \frac{\Delta G^0 \times R}{P} \tag{4}$$

where ΔG^0 is the standard Gibbs energy for the photodegradable substance multiplied by the rate R of fuel formation in moles/second and divided by the incident radiation power. If instead of ΔG^0 we use the corresponding potential, calculated by $E = \Delta G^0/nF$, where n is the number of electrons involved in the photodegradation procedure and F is the Faraday constant, i.e. 96485 C/mol, then

$$\eta = \frac{E \times I}{P} \tag{5}$$

where I is the current involved in the decomposition process. For example, in the case of water splitting $E = 1.23$ V [11,210]. The value of η, when it refers to fuel production by the PEC cell, will be overestimated if I is taken as the current, which is actually measured with an instrument. The safest way is to calculate I by the value, which corresponds to the quantity of fuel produced. Thus if, for example, the device produces 2 μmol/min of hydrogen [136], since two electrons correspond to one H_2, we expect that the corresponding current will be $I = 2$(electrons/molecule) $\times$ $(2 \times 10^{-6}$ mol/60 s$) \times 6.023 \times 10^{23}$ (molecules/mole) $\times 1.602 \times 10^{-19}$ (C/electron) = 6.4 mA. In the case when a bias voltage V_{app} is applied, then Eq. (5) should be substituted by the following equation:

$$\eta = \frac{(E - V_{app}) \times I}{P}. \tag{6}$$

This last model for measuring efficiency [179,210] has been applied in several cases [15,177,184]. The model of Eqs. (5) and (6) is simple and clear. Caution is only necessary to properly define E in each case.

Some authors prefer to employ a model of IQE, adapted to PFCs, to calculate efficiency in the case of organic material decomposition. Thus in Ref. [62], η is given by the following relation:

$$\eta = \frac{N_m \times n}{N_{eff}} \tag{7}$$

where N_m is the number of molecules decomposed in the unit of time, n is the number of electrons involved in the decomposition of each molecule and N_{eff} is the number of effective photons involved in the photodecomposition in the unit of time. Caution is necessary in this model to properly calculate N_{eff}.

7.2. The current doubling effect

The efficiency of PEC cells is sometimes found unusually high. The reason may be the so-called "current doubling" effect [14,79,81,82,213–218]. This effect is due to intermediate radical formation by photoanodic decomposition of organic substances, which inject additional electrons into the conduction band thus increasing current. For example, in the case of methanol [14], the excitation of the semiconductor creates an electron–hole pair. The hole interacts with methanol and creates an unstable methoxy radical:
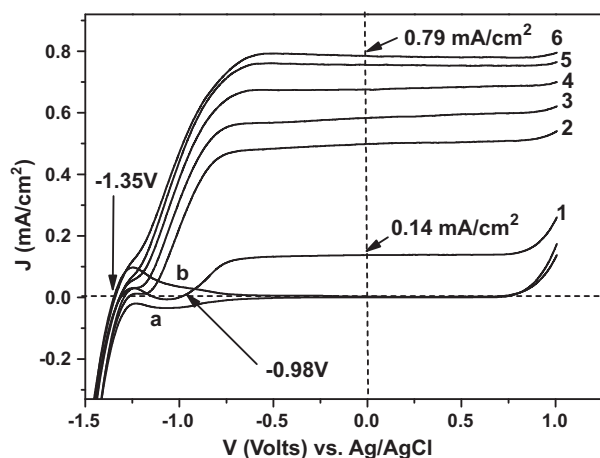
$$CH_3OH + h^+ \rightarrow H_3CO^\bullet + H^+ \tag{XXXII}$$

$$H_3CO^\bullet \rightarrow HCHO + H^+ + e^- \tag{XXXIII}$$

Fig. 10. Variation of the current density *J* with voltage in a three electrode single compartment reactor. The working electrode was FTO bearing nanocrystalline titania [71]. The counter electrode was a carbon cloth bearing a Pt/Carbon-Black electrocatalyst. The electrolyte contained 0.2 M NaOH. Curves 1–6 were recorded under UVA (Black Light) irradiation and correspond to various ethanol volume percentages: (1) 0; (2) 0.1; (3) 1.0; (4) 5; (5) 10; and (6) 20. Curves (a) and (b) were recorded in the dark: (a) in the absence of ethanol and (b) in the presence of 20 v% ethanol.

The electron generated in reaction (XXXIII) is injected into the CB of the photocatalyst. Thus for one photon absorbed, two electrons are found in the CB, one being the photogenerated and the second the injected electron. Hence the "current doubling". Of course, more electrons can be further injected by decomposition of formaldehyde and so on. The current doubling effect cannot be easily separated from simple increase of current due to efficient hole scavenging by the organic agent, especially at high pH, when holes will be also scavenged by OH^-. Let us examine the following data presented by Fig. 10. It is seen that the saturation current increased about three-fold in the presence of 0.1 v% ethanol and increased further upon further ethanol addition. This current increase, more than 5-fold in the presence of 20 v% ethanol, is obviously due to efficient hole scavenging by the reducing agent but incorporation of the current doubling effect is not excluded. We believe that the current doubling effect will unveil itself when unusually high values of efficiency are detected. In this respect, it must be taken into account that, contrary to the case of Fig. 10, all studies dealing with current doubling effect [14,79,81,82,213–218] were carried out in electrolytes of relatively low pH. The reason for that is to avoid high OH^- concentration, since hydroxyl ions would compete with the organic agent for hole scavenging. In conclusion, current doubling may not be easily distinguished from other current-increasing effects but it is expected to uncover itself in cases of unusually high efficiency.

8. Conclusions

This review has shown that a PFC can be easily constructed and can be used to consume an organic substance (i.e. a fuel) to produce electricity, when the photoanode is excited by appropriate radiation. The basic cell configuration has not changed through the years but the design of appropriate cell geometry leaves a lot of room for inspiration. A standard choice of semiconductor photocatalyst is nanocrystalline titania but other semiconductors, like ZnO and non-oxide chalcogenides, as well as combinations of semiconductors make a rich choice of materials to construct photoanodes. Even though, studies on titania are exhaustive, the various titania nanostructures are still studied with a lot of ardour. On the contrary, the choice of electrocatalysts for the cathode electrode is rather lim-

ited but it leaves a lot of space for research. The same is true for the choice of electrolytes. Mechanistic studies for photodegradable fuels for PFCs are mainly known for methanol and ethanol and fewer for glycerol. Studies for higher polyols and sugars may be of interest. The photodegradation route of an organic substance towards its mineralization seems to depend on a delicate balance between the number of electrons flowing through the external load and those that may be available to the photodegradation procedure. A PEC cell that runs with a cathode in the absence of oxygen produces hydrogen. Other fuels may be produced under appropriate conditions as byproducts of the photodegradation process. Therefore, fuel and electricity production may be simultaneous in a PEC cell. However, researchers dealing with this field realize that more hydrogen can be produced by a PC than a PEC operation. Therefore, it seems that a PFC, i.e. a cell designed to produce only electricity, is more effective. All these matters have been studied previously but the still open questions are many and the related work is worth the undertaking.

Acknowledgement

References

[1] A. Fujishima, K. Honda, Electrochemical photolysis of water at a semiconductor electrode, Nature 238 (1972) 37–38.
[2] A.J. Nozik, Photoelectrolysis of water using semiconducting TiO_2 crystals, Nature 257 (1975) 383–386.
[3] J.G. Mavroides, D.I. Tchernev, J.A. Kafalas, D.F. Kolesar, Photoelectrolysis of water in cells with TiO_2 anodes, Mat. Res. Bull. 10 (1975) 1023–1030.
[4] J. Manassen, D. Cahen, G. Hodes, A. Sofer, Electrochemical, solid state, photochemical and technological aspects of photoelectrochemical energy converters, Nature 263 (1976) 97–100.
[5] A.J Nozik, Electrode materials for photoelectrochemical devices, J. Crystal Growth 39 (1977) 200–209.
[6] F. Chojnowski, P. Clechet, J.-R. Martin, J.-M. Herrmann, P. Pichat, Hydrogen production by water photoelectrolysis with a powder semiconductor anode, Chem. Phys. Lett. 84 (1981) 555–559.
[7] A.J. Bard, Design of semiconductor photoelectrochemical systems for solar energy conversion, J. Phys. Chem. 86 (1982) 172–177.
[8] D.E. Aspnes, A. Heller, Photoelectrochemical hydrogen evolution and water-photolyzing semiconductor suspensions: properties of platinum group metal catalyst-semiconductor contacts in air and in hydrogen, J. Phys. Chem. 87 (1983) 4919–4929.
[9] N. Getoff, Photoelectrochemical and photocatalytic methods of hydrogen production: a short review, Int. J. Hydrogen Energy 15 (1990) 407–417.
[10] S.U.M. Khan, J. Akikusa, Photoelectrochemical splitting of water at nanocrystalline n-Fe_2O_3 thin film electrodes, J. Phys. Chem. B 103 (1999) 7184–7189.
[11] T. Bak, J. Nowotny, M. Rekas, C.C. Sorrell, Photo-electrochemical hydrogen generation from water using solar energy. Materials-related aspects, Int. J. Hydrogen Energy 27 (2002) 991–1022.
[12] J.H. Park, S. Kim, A.J. Bard, Novel carbon-doped TiO_2 nanotube arrays with high aspect ratios for efficient solar water splitting, Nano Lett. 6 (2006) 24–28.
[13] M. Kaneko, J. Nemoto, H. Ueno, N. Gokan, K. Ohnuki, M. Horikawa, R. Saito, T. Shibata, Photoelectrochemical reaction of biomass and bio-related compounds with nanoporous TiO_2 film photoanode and O_2-reducing cathode, Electrochem. Commun. 8 (2006) 336–340.
[14] B. Seger, P.V. Kamat, Fuel cell geared in reverse: photocatalytic hydrogen production using a TiO_2/Nafion/Pt membrane assembly with no applied bias, J. Phys. Chem. C 113 (2009) 18946–18952.
[15] R. Tode, A. Ebrahimi, S. Fukumoto, K. Iyatani, M. Takeuchi, M. Matsuoka, C.H. Lee, C.-S. Jiang, M. Anpo, Photocatalytic decomposition of water on double-layered visible light-responsive TiO_2 thin films prepared by a magnetron sputtering deposition method, Catal. Lett. 135 (2010) 10–15.
[16] F. Le Formal, M. Gratzel, K. Sivula, Controlling photoactivity in ultra-thin hematite films for solar water-splitting, Adv. Funct. Mater. 20 (2010) 1099–1107.
[17] M. Antoniadou, D.I. Kondarides, D. Labou, S. Neophytides, P. Lianos, An efficient photoelectrochemical cell functioning in the presence of organic wastes, Sol. Energy Mater. Sol. Cells 94 (2010) 592–597.
[18] S. Borman, Photoelectrochemical cells: energy source for the future, Chem. Eng. News (1991) 17–19.
[19] T. Kawai, T. Sakata, Photocatalytic decomposition of gaseous water over TiO_2 and TiO_2-RuO_2 surfaces, Chem. Phys. Lett. 72 (1980) 87–89.

[20] E. Borganello, J. Kiwi, M. Gratzel, E. Pelizzetti, M. Visca, Visible light induced water cleavage in colloidal solutions of chromium-doped titaniumdioxide particles, J. Am. Chem. Soc. 104 (1982) 2996–3002.

[21] J.-M. Herrmann, J. Disdier, P. Pichat, Effect of chromium doping on the electrical and catalytic properties of powder titania under UV and visible illumination, Chem. Phys. Lett. 108 (1984) 618–621.

[22] M.R. Hoffmann, S.T. Martin, W. Choi, D.W. Bahnemann, Environmental applications of semiconductor photocatalysis, Chem. Rev. 95 (1995) 69–96.

[23] K.E. Karakitsou, X.E. Verykios, Effects of altervalent cation doping of TiO_2 on its performance as a photocatalyst for water cleavage, J. Phys. Chem. 97 (1993) 1184–1189.

[24] M.A. Fox, M.T. Dulay, Heterogeneous photocatalysis, Chem. Rev. 93 (1993) 341–357.

[25] A.L. Linsebigler, G. Lu, J.T. Yates Jr., Photocatalysis on TiO_2 surfaces: principles, mechanisms and selected results, Chem. Rev. 95 (1995) 735–758.

[26] K. Vinodgopal, D.E. Wynkoop, P.V. Kamat, Environmental photochemistry on semiconductor surfaces: photosensitized degradation of textile azo dye, acid orange 7, on TiO_2 particles using visible light, Environ. Sci. Technol. 30 (1996) 1660–1666.

[27] B. Ohtani, K. Iwai, S.-I. Nishimoto, S. Sato, Role of platinum deposits on titanium (IV) oxide particles: structural and kinetic analyses of photocatalytic reaction in aqueous alcohol and amino acid solutions, J. Phys. Chem. B 101 (1997) 3349–3359.

[28] T. Wu, G. Liu, J. Zhao, H. Hidaka, N. Serpone, Photoassisted degradation of dye pollutants. V. Self-photosensitized oxidative transformation of rhodamine B under visible light irradiation in aqueous TiO_2 dispersions, J. Phys. Chem. B 102 (1998) 5845–5851.

[29] A. Sclafani, J.-M. Herrmann, Influence of metallic silver and of platinum-silver bimetallic deposits on the photocatalytic activity of titania (anatase and rutile) in organic and aqueous media, J. Photochem. Photobiol. A: Chem. 113 (1998) 181–188.

[30] N. Negishi, K. Takeuchi, T. Ibusuki, Surface structure of the TiO_2 thin film photocatalyst, J. Mater. Sci. 33 (1998) 5789–5794.

[31] A. Fujishima, T.N. Rao, D.A. Tryk, Titanium dioxide photocatalysis, J. Photochem. Photobiol. C: Photochem. Rev. 1 (2000) 1–21.

[32] E. Vulliet, C. Emmelin, J.-M. Chovelon, C. Guillard, J.-M. Herrmann, Photocatalytic degradation of sulfonylurea herbicides in aqueous TiO_2, Appl. Catal. B: Environ. 38 (2002) 127–137.

[33] A. Di Paola, G. Marci, L. Palmisano, M. Sciavello, K. Uosaki, S. Ikeda, B. Ohtani, Preparation of polycrystalline TiO_2 photocatalysts impregnated with various transition metal ions: Characterization and photocatalytic activity for the degradation of 4-nitrophenol, J. Phys. Chem. B 106 (2002) 637–645.

[34] C. Guillard, B. Beaugiraud, C. Dutriez, J.-M. Herrmann, H. Jaffrezic-Renault, M. Lacroix, Physicochemical properties and photocatalytic activities of TiO_2-films prepeared by sol–gel methods, Appl. Catal. B: Environ. 39 (2002) 331–342.

[35] I.M. Arabatzis, T. Stergiopoulos, D. Andreeva, S. Kitova, S.G. Neophytides, P. Falaras, Characterization and photocatalytic activity of Au/TiO_2 thin films for azo-dye degradation, J. Catal. 220 (2003) 127–135.

[36] S. Nakade, Y. Saito, W. Kubo, T. Kanzaki, T. Kitamura, Y. Wada, S. Yanagida, Enhancement of electron transport in nano-porous TiO_2 electrodes by dye adsorption, Electrochem. Commun. 5 (2003) 804–808.

[37] J.M. Coronado, M.E. Zorn, I. Tejedor-Tejedor, M.A. Anderson, Photocatalytic oxidation of ketones in the gas phase over TiO_2 thin films: a kinetic study on the influence of water vapour, Appl. Catal. B: Environ. 43 (2003) 329–344.

[38] M. Mrowetz, W. Balcerski, A.J. Colussi, M.R. Hoffmann, Oxidative Power of nitrogen-doped TiO_2 photocatalysts under visible illumination, J. Phys. Chem. B 108 (2004) 17269–17273.

[39] I.K. Konstantinou, T.A. Albanis, TiO_2-assisted photocatalytic degradation of azo dyes in aqueous solution: kinetic and mechanistic investigations: a review, Appl. Catal. B: Environ. 49 (2004) 1–14.

[40] M. Kositzi, I. Poulios, S. Malato, J. Caceres, A. Campos, Solar photocatalytic treatment of synthetic municipal wastewater, Water Res. 38 (2004) 1147–1154.

[41] Q. Yang, D.D. Dionysiou, Photolytic degradation of chlorinated phenols in room temperature ionic liquids, J. Photochem. Photobiol. A: Chem. 165 (2004) 229–240.

[42] J. Zhu, F. Chen, J. Zhang, H. Chen, M. Anpo, Fe^{3+}-TiO_2 photocatalysts prepared by combining sol–gel method with hydrothermal treatment and their characterization, J. Photochem. Photobiol. A: Chem. 180 (2006) 196–204.

[43] A. Patsoura, D.I. Kondarides, X.E. Verykios, Enhancement of photoinduced hydrogen production from irradiated Pt/TiO_2 suspensions with simultaneous degradation of azo-dyes, Appl. Catal. B: Environ. 64 (2006) 171–179.

[44] W. Bahnemann, M. Muneer, M.M. Haque, Titanium dioxide-mediated photocatalysed degradation of few selected organic pollutants in aqueous suspensions, Catal. Today 124 (2007) 133–148.

[45] A. Fujishima, X. Zhang, D.A. Tryk, TiO_2 photocatalysis and related surface phenomena, Surf. Sci. Rep. 63 (2008) 515–582.

[46] K. Pelentridou, E. Stathatos, H. Karasali, P. Lianos, Photodegradation of the herbicide azimsulfuron using nanocrystalline titania films as photocatalyst and low intensity black light radiation or simulated solar radiation as excitation source, J. Hazard. Mater. 163 (2009) 756–760.

[47] M. Kawai, T. Kawai, S. Naito, K. Tamaru, The mechanism of photocatalytic reaction over Pt/TiO_2: Production of H_2 and aldehyde from gaseous alcohol and water, Chem. Phys. Lett. 110 (1984) 58–62.

[48] T. Sakata, T. Kawai, Heterogeneous photocatalytic production of hydrogen and methane from ethanol and water, Chem. Phys. Lett. 80 (1981) 341–344.

[49] S. Nakabayashi, A. Fujishima, K. Honda, Experimental evidence for the hydrogen evolution site in photocatalytic process on Pt/TiO_2, Chem. Phys. Lett. 102 (1983) 464–465.

[50] G.R. Bamwenda, S. Tsubota, T. Nakamura, M. Haruta, Photoassisted hydrogen production from a water-ethanol solution: a comparison of activities of Au-TiO_2 and Pt-TiO_2, J. Photochem. Photobiol. A: Chem. 89 (1995) 177–189.

[51] G.C. De, A.M. Roy, S.S. Bhattacharya, Photocatalytic production of hydrogen and concomitant cleavage of industrial waste hydrogen sulphide, Int. J. Hydrogen Energy 20 (1995) 127–131.

[52] M. Ashokkumar, An overview on semiconductor particulate systems for photoproduction of hydrogen, Int. J. Hydrogen Energy 23 (1998) 427–438.

[53] A.A. Nada, M.H. Barakat, H.A. Hamed, N.R. Mohamed, T.N. Veziroglu, Studies on the photocatalytic hydrogen production using suspended modified TiO_2 photocatalysts, Int. J. Hydrogen Energy 30 (2005) 687–691.

[54] A. Galinska, J. Walendziewski, Photocatalytic water splitting over $Pt-TiO_2$ in the presence of sacrificial reagents, Energy Fuels 19 (2005) 1143–1147.

[55] M. Li, Y. Li, S. Peng, G. Lu, S. Li, Photocatalytic hydrogen generation using glycerol wastewater over Pt/TiO_2, Front. Chem. Chin. 4 (2009) 32–38.

[56] D.I. Kondarides, V.M. Daskalaki, A. Patsoura, X.E. Verykios, Hydrogen production by photo-induced reforming of biomass components and derivatives at ambient conditions, Catal. Lett. 122 (2008) 26–32.

[57] Y. Mizukoshi, Y. Makise, T. Shuto, J. Hu, A. Tominaga, S. Shironita, S. Tanabe, Immobilization of noble metal nanoparticles on the surface of TiO_2 by the sonochemical method: photocatalytic production of hydrogen from an aqueous solution of ethanol, Ultrason. Sonochem. 14 (2007) 387–392.

[58] N. Strataki, V. Bekiari, D.I. Kondarides, P. Lianos, Hydrogen production by photocatalytic alcohol reforming employing highly efficient nanocrystalline titania films, Appl. Catal. B Environ. 77 (2007) 184–189.

[59] V.M. Daskalaki, D.I. Kondarides, Efficient production of hydrogen by photo-induced reforming of glycerol at ambient conditions, Catal. Today 144 (2009) 75–80.

[60] S. Bae, J. Kang, E. Shim, J. Yoon, H. Joo, Correlation of electrical and physical properties of photoanode with hydrogen evolution in enzymatic photoelectrochemical cell, J. Power Sources 179 (2008) 863–869.

[61] H. Ueno, J. Nemoto, K. Ohnuki, M. Horikawa, M. Hoshino, M. Kaneko, Photoelectrochemical reaction of biomass-related compounds in a biophotochemical cell comprising a nanoporous TiO_2 film photoanode and an O_2-reducing cathode, J. Appl. Electrochem. 39 (2009) 1897–1905.

[62] M. Kaneko, H. Ueno, R. Saito, S. Yamaguchi, Y. Fujii, J. Nemoto, UV light-activated decomposition/cleaning of concentrated biomass wastes involving also solid suspensions with remarkably high quantum efficiency, Appl. Catal. B Environ. 91 (2009) 254–261.

[63] M. Kaneko, H. Ueno, R. Saito, J. Nemoto, Highly efficient photoelectrocatalytic decomposition of biomass compounds using a nanoporous semiconductor photoanode and an O_2-reducing cathode with quantum efficiency over 100, Catal. Lett. 131 (2009) 184–188.

[64] M. Kaneko, H. Ueno, R. Saito, S. Suzuki, J. Nemoto, Y. Fujii, Biophotochemical cell (BPCC) to photodecompose biomass and bio-related compounds by UV irradiation with simultaneous electrical power generation, J. Photochem. Photobiol. A: Chem. 205 (2009) 168–172.

[65] M. Canterino, I.D. Somma, R. Marotta, R. Andreozzi, V. Caprio, Energy recovery in wastewater decontamination: simultaneous photocatalytic oxidation of an organic substrate and electricity generation, Water Res. 43 (2009) 2710–2716.

[66] J. Nowotny, C.C. Sorrell, L.R. Sheppard, T. Bak, Solar-hydrogen: Enviromentally safe fuel for the future, Int. J. Hydrogen Energy 30 (2005) 521–544.

[67] P.V. Kamat, Meeting the clean energy demand: nanostructure architectures for solar energy conversion, J. Phys. Chem. C 111 (2007) 2834–2860.

[68] T.-H. Kim, M. Saito, M. Matsuoka, S. Tsukada, K. Wada, M. Anpo, Photocatalytic oxidation of ethanethiol on a photoelectrochemical circuit system consisting of a rod-type TiO_2 electrode and a silicon solar cell, Res. Chem. Intermed. 35 (2009) 633–642.

[69] J. Brillet, M. Cornuz, F.L. Formal, J.-H. Yum, M. Gratzel, K. Sivula, Examining architectures of photoanode-photovoltaic tandem cells for solar water splitting, J. Mater. Res. 25 (2010) 17–24.

[70] E.L. Miller, R.E. Rocheleau, X.M. Deng, Design considerations for a hybrid amorphous silicon/photoelectrochemical multijunction cell for hydrogen production, Int. J. Hydrogen Energy 28 (2003) 615–623.

[71] M. Antoniadou, P. Lianos, Production of electricity by photoelectrochemical oxidation of ethanol in a photofuelcell, Appl. Catal. B: Environ. 99 (2010) 307–313.

[72] M. Boehme, C. Charton, Properties of ITO on PET film in dependence on the coating conditions and thermal processing, Surf. Coat. Technol. 200 (2005) 932–935.

[73] A.J. Nozik, R. Memming, Physical chemistry of semiconductor-liquid interfaces, J. Phys. Chem. 100 (1996) 13061–13078.

[74] M. Miyauchi, A. Nakajima, T. Watanabe, K. Hashimoto, Photocatalysis and photoinduced hydrophilicity of various metal oxide thin films, Chem. Mater. 14 (2002) 2812–2816.

[75] S. Sakthivel, B. Neppolian, M.V. Shankar, B. Arabindoo, M. Palanichamy, V. Murugesan, Solar photocatalytic degradation of azo dye: comparison of photocatalytc efficiency of ZnO and TiO_2, Solar Energy Mater. Sol. Cells 77 (2003) 65–82.

[76] J.-M. Herrmann, Heterogeneous photocatalysis: state of the art and present applications, Top. Catal. 34 (2005) 49–65.

[77] I. Poulios, I. Tsachpinis, Photodegradation of the textile dye Reactive Black 5 in the presence of semiconducting oxides, J. Chem. Technol. Biotechnol. 74 (1999) 349–357.

[78] I. Poulios, A. Avranas, E. Rekliti, A. Zouboulis, Photocatalytic oxidation of Auramine O in the presence of semiconducting oxides, J. Chem. Technol. Biotechnol. 75 (2000) 205–212.

[79] A. Fujishima, T. Kato, E. Maekawa, K. Honda, Mechanism of the current doubling effect. I. The ZnO photoanode in aqueous solution of sodium formate, Bull. Chem. Soc. Jpn. 54 (1981) 1671–1674.

[80] C.M. Janet, S. Navaladian, B. Viswanathan, T.K. Varadarajan, R.P. Viswanath, Heterogeneous wet chemical synthesis of superlattice-type hierarchical ZnO architectures for concurrent H_2 production and reduction, J. Phys. Chem. C 114 (2010) 2622–2632.

[81] J.-S. Lee, T. Kato, A. Fujishima, K. Honda, Photoelectrochemical oxidation of alcohols on polycrystalline zinc oxide, Bull. Chem. Soc. Jpn. 57 (1984) 1179–1183.

[82] S.R. Morrison, T. Freund, Chemical role of holes and electrons in ZnO photocatalysis, J. Chem. Phys. 47 (1967) 1543–1551.

[83] T. Yoshida, T. Pauporte, D. Lincot, T. Oekermann, H. Minoura, Cathodic electrodeposition of ZnO/Eosin Y hybrid thin films from oxygen-saturated aqueous solution of $ZnCl_2$ and Eosin Y, J. Electrochem. Soc. 150 (2003) C608–C615.

[84] K. Nonomura, D. Komatsu, T. Yoshida, H. Minoura, D. Schlettwein, Dependence of the photoelectrochemical performance of sensitized ZnO on the crystalline orientation in electrodeposited ZnO thin films, Phys. Chem. Chem. Phys. 9 (2007) 1843–1849.

[85] T. Loewenstein, A. Hastall, M. Mingebach, Y. Zimmermann, A. Neudeck, D. Schlettwein, Textile electrodes as substrates for the electrodeposition of porous ZnO, Phys. Chem. Chem. Phys. 10 (2008) 1844–1847.

[86] F.C. Krebs, Y. Thomann, R. Thomann, J.W. Andreasen, A simple nanostructured polymer/ZnO hybrid solar cell-preparation and operation in air, Nanotechnology 19 (2008) 1–12.

[87] C. Pacholski, A. Kornowski, H. Weller, Self-assembly of ZnO: from nanodots to nanorods, Angew. Chem. Int. Ed. 41 (2002) 1188–1191.

[88] J.L. Yang, S.J. An, W.I. Park, G.-C. Yi, W. Choi, Photocatalysis using ZnO thin films and nanoneedles grown by metal-organic chemical vapor deposition, Adv. Mater. 16 (2004) 1661–1664.

[89] D.C. Olson, J. Piris, R.T. Collins, S.E. Shaheen, D.S. Ginley, Hybrid photovoltaic devices of polymer and ZnO nanofiber composites, Thin Solid Films 496 (2006) 26–29.

[90] M. Law, L.E. Greene, J.C. Johnson, R. Saykally, P. Yang, Nanowire dye-sensitized solar cells, Nat. Mater. 4 (2005) 455–459.

[91] K. Sivula, R. Zboril, F.L. Formal, R. Robert, A. Weidenkaff, J. Tucek, J. Frydrych, M. Gratzel, Photoelectrochemical water splitting with mesoporous hematite prepared by a solution-based colloidal approach, J. Am. Chem. Soc. 132 (2010) 7436–7444.

[92] S.A. Majumder, S.U.M. Khan, Photoelectrolysis of water at bare and electrocatalyst covered thin film iron oxide electrode, Int. J. Hydrogen Energy 19 (1994) 881–887.

[93] (a) M. Fujii, T. Kawai, S. Kawai, Photocatalytic activity and the energy levels of electrons in a semiconductor particle under irradiation, Chem. Phys. Lett. 106 (1984) 517–522;
(b) P.V. Kamat, N.M. Dimitrijevic, Colloidal semiconductors as photocatalysts for solar energy conversion, Solar Energy 44 (1990) 83–98.

[94] (a) P.M. Wood, The two redox potentials for oxygen reduction to superoxide, Trends Biochem. Sci. 12 (1987) 250–251;
(b) P.M. Paul, The potential diagram for oxygen at pH 7, Biochem. J. 253 (1988) 287–289.

[95] N. Serpone, P. Maruthamuthu, P. Pichat, E. Pelizzetti, H. Hidaka, Exploiting the interparticle electron transfer process in the photocatalysed oxidation of phenol, 2-chlorophenol and pentachlorophenol: chemical evidence for electron and hole transfer between coupled semiconductors, J. Photochem. Photobiol. A: Chem. 85 (1995) 247–255.

[96] V.L. Kuznetsov, P.P. Edwards, Function materials for sustainable energy technologies: four case studies, Chem. Sus. Chem. 3 (2010) 44–58.

[97] K. Kalyanasundaram, E. Borganello, M. Gratzel, Visible light induced water cleavage in CdS dispersions loaded with Pt and RuO_2, hole scavenging by RuO_2, Helv. Chim. Acta 64 (1981) 362–366.

[98] M. Matsumura, Y. Saho, H. Tsubomura, Photocatalytic hydrogen production from solutions of sulfite using platinized cadmium sulfide powder, J. Phys. Chem. 87 (1983) 3807–3808.

[99] J.R. Harbour, R. Wolkow, M.L. Hair, Effect of platinization on the photoproperties of CdS pigments in dispersion. Determination by H_2 evolution, O_2 uptake and electron spin resonance spectroscopy, J. Phys. Chem. 85 (1981) 4029–14029.

[100] M. Meyer, C. Wallberg, K. Kurihara, J.H. Fendler, Photosensitized charge separation and hydrogen production in reversed micelle entrapped platinized colloidal cadmium sulphide, J. Chem. Soc. Chem. Commun. 2 (1984) 90–91.

[101] N. Buhler, K. Meier, J.-F. Reber, Photochemical hydrogen production with cadmium sulfide suspensions, J. Phys. Chem. 88 (1984) 3261–3268.

[102] M. Matsumura, S. Furukawa, Y. Saho, H. Tsubomura, Cadmium sulfide photocatalyzed hydrogen production from aqueous solutions of sulfite: Effect of crystal structure and preparation method of the catalyst, J. Phys. Chem. 89 (1985) 1327–1329.

[103] J.-F. Reber, K. Meier, Photochemical production of hydrogen with zinc sulfide suspensions, J. Phys. Chem. 88 (1984) 5903–5913.

[104] M. Barbeni, E. Pelizzetti, E. Borganello, N. Serpone, M. Gratzel, L. Balducci, M. Visca, Hydrogen from hydrogen sulfide cleavage. Improved efficiencies via modification of semiconductor particulates, Int. J. Hydrogen Energy 10 (1985) 249–253.

[105] N. Kakuta, K.H. Park, M.F. Finlayson, A. Ueno, A.J. Bard, A. Campion, M.A. Fox, S.E. Webber, J.M. White, Photoassisted hydrogen production using visible light and coprecipitated ZnS-CdS without a noble metal, J. Phys. Chem. 89 (1985) 732–734.

[106] A. Ueno, N. Kakuta, K.H. Park, M.F. Finlayson, A.J. Bard, A. Campion, M.A. Fox, S.E. Webber, J.M. White, Silica-supported ZnS-CdS mixed semiconductor catalysts for photogeneration of hydrogen, J. Phys. Chem. 89 (1985) 3828–3833.

[107] O. Enea, A.J. Bard, Photoredox reactions at semiconductor particles incorporated into clays. CdS and ZnS + CdS mixtures in colloidal montmorillonite suspensions, J. Phys. Chem. 90 (1986) 301–306.

[108] D.N. Furlong, F. Grieser, D. Hayes, R. Hayes, W. Sasse, D. Wells, Kinetics of hydrogen production from illuminated $CdS/Pt/Na_2S$ dispersions, J. Phys. Chem. 90 (1986) 2388–2396.

[109] K. Hara, K. Sayama, H. Arakawa, Photocatalytic hydrogen and oxygen formation over SiO_2-supported RuS_2 in the presence of sacrificial donor and acceptor, Appl. Catal. A: General 189 (1999) 127–137.

[110] N. Bao, L. Shen, T. Takata, K. Domen, A. Gupta, K. Yanagisawa, C.A. Grimes, Facile Cd-Thiourea complex thermolysis synthesis of phase-controlled CdS nanocrystals for photocatalytic hydrogen production under visible light, J. Phys. Chem. C 111 (2007) 17527–17534.

[111] J.S. Jang, U.A. Joshi, J.S. Lee, Solvothermal synthesis of CdS nanowires for photocatalytic hydrogen and electricity production, J. Phys. Chem. C 111 (2007) 13280–13287.

[112] H. Yan, J. Yang, G. Ma, G. Wu, X. Zong, Z. Lei, J. Shi, C. Li, Visible-light-driven hydrogen production with extremely high quantum efficiency on Pt-PdS/CdS photocatalyst, J. Catal. 266 (2009) 165–168.

[113] W. Zhang, R. Xu, Surface engineered active photocatalysts without noble metals: $CuS-Zn_xCd_{1-x}S$ nanospheres by one-step synthesis, Int. J. Hydrogen Energy 34 (2009) 8495–8503.

[114] X. Wang, K. Shih, X.Y. Li, Photocatalytic hydrogen generation from water under visible light using core/shell nano-catalysts, Water Sci. Techn. 61 (2010) 2303–2308.

[115] A. Deshpande, N.M. Gupta, Critical role of particle size and interfacial properties in the visible light induced splitting of water over the nanocrystallites of supported cadmium sulphide, Int. J. Hydrogen Energy 35 (2010) 3287–3296.

[116] L. Amirav, A.P. Alivisatos, Photocatalytic hydrogen production with tunable nanorod heterostructures, J. Phys. Chem. Lett. 1 (2010) 1051–1054.

[117] X. Zong, G. Wu, H. Yan, G. Ma, J. Shi, F. Wen, L. Wang, C. Li, Photocatalytic H_2 evolution on MoS_2/CdS catalysts under visible light irradiation, J. Phys. Chem. C 114 (2010) 1963–1968.

[118] C-H.J. Liu, J. Olsen, D.R. Saunders, J.H. Wang, Photoactivation of CdSe films for photoelectrochemical cells, J. Electrochem. Soc. 128 (1981) 1224–1228.

[119] M.F. Finlayson, B.L. Wheeler, N. Kakuta, K.-H. Park, A.J. Bard, A. Campion, M.A. Fox, S.E. Webber, J.M. White, Determination of flat-band position of CdS crystals, films and powders by photocurrent and impedance techniques. Photoredox reaction mediated by intragap states, J. Phys. Chem. 89 (1985) 5676–5681.

[120] D. Cahen, Y. Mirovsky, Ternary chalcogenide-based photoelectrochemical cells. 6. Is there a thermodynamic explanation for the output stability of $CuInS_2$ and $CuInSe_2$ photoanodes? J. Phys. Chem. 89 (1985) 2818–2827.

[121] H. Ti Tien, Z.-C. Bi, A.K. Tripathi, Photoresponses of semiconductor polycrystallites separating two aqueous solutions, Photochem. Photobiol. 44 (1986) 779–783.

[122] A.K. Tripathy, H. Ti Tien, Dual electrolyte-semiconductor contact CdSe electrochemical photocell, J. Appl. Electrochem. 17 (1987) 1100–1103.

[123] E.S. Smotkin, S. Cervera-March, A.J. Bard, A. Campion, M.A. Fox, T. Mallouk, S.E. Webber, J.M. White, Bipolar CdSe/CoS semiconductor photoelectrode arrays for unassisted photolytic water splitting, J. Phys. Chem. 91 (1987) 6–8.

[124] D. Lincot, J. Vedel, Adsorption of telluride ions on cadmium telluride. Consequences for photoelectrochemical cells, J. Phys. Chem. 92 (1988) 4103–4110.

[125] G. Hodes, J. Manassen, D. Cahen, Photoelectrochemical energy conversion and storage using polycrystalline chalcogenide electrodes, Nature 261 (1976) 403–404.

[126] H. Ti Tien, J.-W. Chen, Hydrogen generation from artificial sea water in a semiconductor septum electrochemical photovoltaic cell, Photochem. Photobiol. 49 (1989) 527–530.

[127] A.M. Roy, G.C. De, N. Sasmal, S.S. Bhattacharyya, Determination of the flat-band potential of semiconductor particles in suspension by photovoltage measurement, Int. J. Hydrogen Energy 20 (1995) 627–630.

[128] G. Milczarek, A. Kasuya, S. Mamykin, T. Arai, K. Shinoda, K. Tohji, Optimization of a two-compartment photoelectrochemical cell for solar hydrogen production, Int. J. Hydrogen Energy 28 (2003) 919–926.

[129] R.G. Bhattacharyya, D.P. Mandal, S.C. Bera, K.K. Rohatgi-Mukherjee, Photoelectrosynthesis of dihydrogen via water-splitting using S_x^{2-} ($x = 1,2,3...$) as an anolyte: a first step for a viable solar rechargeable battery, Int. J. Hydrogen Energy 21 (1996) 343–347.

[130] M. Gunasekaran, R. Gopalakrishnan, R. Sivakumar, P. Ramasamy, M. Ichimura, Deposition of cadmium sulphide and cadmium zinc sulphide thin films by photochemical deposition and their characterisation, Surf. Eng. 22 (2006) 73–77.

[131] C.-F. Chi, S.-Y. Liau, Y.-L. Lee, The heat annealing effect on the performance of CdS/CdSe-sensitized TiO₂ photoelectrodes in photochemical hydrogen generation, Nanotechnology 21 (2010) 025202.

[132] X.-M. Song, J.-M. Wu, M. Yan, Distinct visible-light response of composite films with CdS electrodeposited on TiO₂ nanorod and nanotube arrays, Electrochem. Commun. 11 (2009) 2203–2206.

[133] Y.-L. Lee, C.-F. Chi, S.-Y. Liau, CdS/CdSe Co-sensitized TiO₂ photoelectrode for efficient hydrogen generation in a photoelectrochemical cell, Chem. Mater. 22 (2010) 922–927.

[134] G. Wang, X. Yang, F. Qian, J.Z. Zhang, Y. Li, Double-sized CdS and CdSe quantum dot co-sensitized ZnO nanowire arrays for photoelectrochemical hydrogen generation, Nano Lett. 10 (2010) 1088–1092.

[135] J. Bai, J. Li, Y. Liu, B. Zhou, W. Cai, A new glass substrate photoelectrocatalytic electrode for efficient visible-light hydrogen production: CdS sensitized TiO₂ nanotube arrays, Appl. Catal. B: Environ. 95 (2010) 408–413.

[136] M. Antoniadou, P. Lianos, Near ultraviolet and visible light photoelectrochemical degradation of organic substances producing electricity and hydrogen, J. Photochem. Photobiol. A: Chem. 204 (2009) 69–74.

[137] N. Strataki, M. Antoniadou, V. Dracopoulos, P. Lianos, Visible-light photocatalytic hydrogen production from ethanol–water mixtures using a Pt-CdS-TiO₂ photocatalyst, Catal. Today 151 (2010) 53–57.

[138] B.O. Dabbousi, J. Rodriguez-Viejo, F.V. Mikulec, J.R. Heine, H. Mattousi, R. Ober, K.F. Jensen, M.G. Bawendi, (CdSe)ZnS core-shell quantum dots: synthesis and characterization of a size series of highly luminescent nanocrystallites, J. Phys. Chem. B 101 (1997) 9463–9475.

[139] H. Jia, H. Xu, Y. Hu, Y. Tang, L. Zhang, TiO₂@CdS core-shell nanorods films: fabrication and dramatically enhanced photoelectrochemical properties, Electrochem. Commun. 9 (2007) 354–360.

[140] G. Dukovic, M.G. Merkle, J.H. Nelson, S.M. Hughes, A.P. Alivisatos, Photodeposition of Pt on colloidal CdS and CdSe/CdS semiconductor nanostructures, Adv. Mater. 20 (2008) 4306–4311.

[141] L. Wang, H. Wei, Y. Fan, X. Liu, J. Zhan, Synthesis, optical properties and photocatalytic activity of one–dimensional CdS@ZnS core-shell nanocomposites, Nanoscale Res. Lett. 4 (2009) 558–564.

[142] X. Wang, G. Liu, G.Q. Lu, H.-M. Cheng, Stable photocatalytic hydrogen evolution from water over ZnO-CdS core-shell nanorods, Int. J. Hydrogen Energy 35 (2010) 8199–8205.

[143] A. Henglein, M. Gutierrez, Photochemistry of colloidal metal sulfides. 5. Fluorescence and chemical reactions of ZnS and ZnS/CdS Co-colloids, Ber. Bunseges. Phys. Chem. 87 (1983) 852–858.

[144] U.G. Akpan, B.H. Hameed, The advancements in sol–gel method of doped-TiO₂ photocatalysts, Appl. Catal. A: General 375 (2010) 1–11.

[145] M. Lim, Y. Zhou, L. Wang, V. Rudolph, G.Q. (Max) Lu, Development and potential of new generation photocatalytic systems for air pollution abatement: an overview, Asia-Pc. J. Chem. Eng. 4 (2009) 387–402.

[146] F. Han, V.S.R. Kambala, M. Srinivasan, D. Rajarathnam, R. Naidu, Tailored titanium dioxide photocatalysts for the degradation of organic dyes in wastewater treatment: a review, Appl. Catal. A: General 359 (2009) 25–40.

[147] Y. Cui, H. Du, L. Wen, Doped-TiO₂ photocatalysts and synthesis methods to prepare TiO₂ films, J. Mater. Sci. Technol. 24 (2008) 675–689.

[148] B.D. Alexander, P.J. Kulesza, I. Rutkowska, R. Solarska, J. Augustynski, Metal oxide photoanodes for solar hydrogen production, J. Mater. Chem. 18 (2008) 2298–2303.

[149] P. Ji, M. Takeuchi, T.-M. Cuong, J. Zhang, M. Matsuoka, M. Anpo, Recent advances in light-responsive titanium oxide-based photocatalysts, Res. Chem. Intermed. 36 (2010) 327–347.

[150] P. Bouras, E. Stathatos, P. Lianos, Pure versus metal-ion-doped nanocrystalline titania for photocatalysis, Appl. Catal. B: Environ. 73 (2007) 51–59.

[151] A.B. Murphy, Band-gap determination from diffuse reflectance measurements of semiconductor film, and application to photoelectrochemical water-splitting, Sol, Energy Mater. Sol. Cells 91 (2007) 1326–1337.

[152] H. Yamashita, M. Harada, J. Misaka, M. Takeuchi, B. Neppolian, M. Anpo, Photocatalytic degradation of organic compounds diluted in water using visible light-responsive metal ion-implanted TiO₂ catalysts: Fe ion-implanted TiO₂, Catal. Today 84 (2003) 191–196.

[153] S.U.M. Khan, M. Al-Shahry, W.B. Ingler Jr., Efficient photochemical water splitting by a chemically modified n-TiO₂, Science 297 (2002) 2243–2245.

[154] C. Hagglund, M. Gratzel, B. Kasemo, Comment on "Efficient photochemical water splitting by a chemically modified n-TiO₂" (II), Science 301 (2003) 1673b.

[155] K. Noworyta, J. Augustynski, Spectral photoresponses of carbon-doped TiO₂ films electrodes, Electrochem. Solid-State Lett. 7 (2004) E31–E33.

[156] B. Neumann, P. Bogdanoff, H. Tributsch, S. Sakthivel, H. Kisch, Electrochemical mass spectroscopic and surfaces photovoltage studies of catalytic water photooxidation by undoped and carbon-doped titania, J. Phys. Chem. B 109 (2005) 16579–16586.

[157] R. Beranek, B. Neumann, S. Sakthivel, M. Janczarek, T. Dittrich, H. Tributsch, H. Kisch, Exploring the electronic structure of nitrogen-modified TiO₂ photocatalysts through photocurrent and surface photovoltage studies, Chem. Phys. 339 (2007) 11–19.

[158] R. Asahi, T. Morikawa, T. Ohwaki, K. Aoki, Y. Taga, Visible-light photocatalysis in nitrogen-doped titanium oxides, Science 293 (2001) 269–271.

[159] N. Strataki, N. Boukos, F. Paloukis, S.G. Neophytides, P. Lianos, Effect of the conditions of platinum deposition on titania nanocrystalline films on the efficiency of photocatalytic oxidation of ethanol and production of hydrogen, Photochem. Photobiol. Sci. 8 (2009) 639–643.

[160] K. Vinodgopal, I. Bedja, P.V. Kamat, Nanostructured semiconductor films for photocatalysis. Photoelectrochemical behavior of SnO₂/TiO₂ composite systems and its role in photocatalytic degradation of a textile azo dye, Chem. Mater. 8 (1996) 2180–2187.

[161] K. Tennakone, J. Bandara, Photocatalytic activity of dye-sensitized tin (IV) oxide nanocrystalline particles attached to zinc oxide particles: long distance electron transfer via ballistic transport of electrons across nanocrystallites, Appl. Catal. A: General 208 (2001) 335–341.

[162] M. Miyauchi, A. Nakajima, T. Watanabe, K. Hashimoto, Photoinduced hydrophilic conversion of TiO₂/WO₃ layered thin films, Chem. Mater. 14 (2002) 4714–4720.

[163] Q. Liu, X. Wu, B. Wang, Q. Liu, Preparation and super-hydrophilic properties of TiO₂/SnO₂ composite thin films, Mater. Res. Bull. 37 (2002) 2255–2262.

[164] S. Pilkenton, D. Raftery, Solid-state NMR studies of the adsorption and photooxidation of ethanol on mixed TiO₂-SnO₂ photocatalysts, Solid State Nucl. Magn. Reson. 24 (2003) 236–253.

[165] D. Li, H. Haneda, Photocatalysis of sprayed nitrogen-containing Fe₂O₃-ZnO and WO₃-ZnO composite powders in gas-phase acetaldehyde decomposition, J. Photochem. Photobiol. A:Chem. 160 (2003) 203–212.

[166] D. Li, H. Haneda, N. Ohashi, S. Hishita, Y. Yoshikawa, Synthesis of nanosized nitrogen-containing MOₓ-ZnO (M = W, V, Fe) composite powders by spray pyrolysis and their visible-light-driven photocatalysis in gas-phase acetaldehyde decomposition, Catal. Today 93–95 (2004) 895–901.

[167] W.-W. Wang, Y.-J. Zhu, L.-X. Yang, ZnO-SnO₂ hollow spheres and hierarchical nanosheets: hydrothermal preparation, formation mechanism and photocatalytic properties, Adv. Funct. Mater. 17 (2007) 59–64.

[168] K.K. Akurati, A. Vital, J.-P. Dellemann, K. Michalow, T. Graule, D. Ferri, A. Baiker, Flame-made WO₃/TiO₂ nanoparticles: relation between surface acidity, structure and photocatalytic activity, Appl. Catal. B: Environ. 79 (2008) 53–62.

[169] H. Wang, S. Baek, J. Lee, S. Lim, High photocatalytic activity of silver-loaded ZnO-SnO₂ coupled catalysts, Chem. Eng. J. 146 (2009) 355–361.

[170] B.-H. Yao, L.-M. Wang, C. Wang, Y.-X. Wang, G.-Y. Zhao, Preparation and performances of RuO₂/TiO₂ films photocatalyst supported on float pearls, Chin. J. Chem. Phys. 20 (2007) 789–795.

[171] P.A. Kolinko, D.V. Kozlov, Products distribution during the gas phase photocatalytic oxidation of ammonia over the various titania based photocatalysts, Appl. Catal. B: Environ. 90 (2009) 126–131.

[172] Y.-L. Gao, Q.-Y. Chen, H.-Z. Tong, H.-P. Hu, D. Qian, Y.-H. Yang, J.-L. Zhou, Preparation of TiO₂ photocatalyst loaded with V₂O₅ for O₂ evolution, J. Centr. South Univ. Technol. 16 (2009) 0919–0925.

[173] T. Mongkhonsi, L. Kershenbaum, The effect of deactivation of a V₂O₅/TiO₂ (anatase) industrial catalyst on reactor behaviour during the partial oxidation of o-xylene to phthalic anhydride, Appl. Catal. A: General 170 (1998) 33–48.

[174] H. Lee, H.C. Leventis, S.-J. Moon, P. Chen, S. Ito, S.A. Haque, T. Torres, F. Nuesch, T. Geiger, S.M. Zakeeruddin, M. Gratzel, Md.K. Nazeeruddin, PbS and CdS quantum dot-sensitized solid-state solar cells: "Old concepts, new results", Adv. Funct. Mater. 19 (2009) 2735–2742.

[175] K. Shankar, G.K. Mor, H.E. Prakasam, O.K. Varghese, C.A. Grimes, Self-assembled hybrid polymer-TiO nanotube array heterojunction solar cells, Langmuir 23 (2007) 12445–12449.

[176] A. Ghicov, H. Tsuchiya, J.M. Macak, P. Schmuki, Titanium oxide nanotubes prepared in phosphate electrolytes, Electrochem. Commun. 7 (2005) 505–509.

[177] S.K. Mohapatra, M. Misra, V.K. Mahajan, K.S. Raja, Design of a highly efficient photoelectrolytic cell for hydrogen generation by water splitting: application of TiO₂₋ₓCₓ nanotube as a photoanode and Pt/TiO₂ nanotubes as a cathode, J. Phys. Chem. C 111 (2007) 8677–8685.

[178] R. Beranek, J.M. Macak, M. Gartner, K. Meyer, P. Schmuki, Enhanced visible light photocurrent generation at surface-modified TiO₂ nanotubes, Electrochim. Acta 54 (2009) 2640–2646.

[179] K. Schankar, J.I. Basham, N.K. Allam, O.K. Varghese, G.K. Mor, X. Feng, M. Paulose, J.A. Seabold, K.S. Choi, C.A. Grimes, Recent advances in the use of TiO2 nanotube and nanowire arrays for oxidative photoelectrochemistry, J. Phys. Chem. C 113 (2009) 6327–6359.

[180] T. Kasuga, M. Hiramatsu, A. Hoson, T. Sekino, K. Niihara, Titania nanotubes prepared by chemical processing, Adv. Mater. 11 (1999) 1307–1311.

[181] B.D. Yao, Y.F. Chan, X.Y. Zhang, W.F. Zhang, Z.Y. Yang, N. Wang, Formation mechanism of TiO₂ nanotubes, Appl. Phys. Lett. 82 (2003) 281–283.

[182] Z.J. Wang, S.C. Qu, X.B. Zeng, J.P. Liu, C.S. Zhang, F.R. Tan, L. Jin, Z.G. Wang, Hybrid bulk heterojunction solar cells from a blend of poly(3-hexylthiophene) and TiO₂ nanotubes, Appl. Surf. Sci. 255 (2008) 1916–1920.

[183] Y. Wu, M. Long, W. Cai, S. Dai, C. Chen, D. Wu, J. Bai, Preparation of photocatalytic anatase nanowire films by in situ oxidation of titanium plate, Nanotechnology 20 (2009) 185703.

[184] M. Matsuoka, M. Kitano, S. Fukumoto, K. Iyatani, M. Takeuchi, M. Anpo, The effect of the hydrothermal treatment with aqueous NaOH solution on the photocatalytic and photoelectrochemical properties of visible light-responsive TiO₂ thin films, Catal. Today 132 (2008) 159–164.

[185] D. Li, Y. Xia, Direct fabrication of composite and ceramic hollow nanofibers by electrospinning, Nano Lett. 4 (2004) 933–938.

[186] Y. Wang, W. Jia, T. Strout, A. Schempf, H. Zhang, B. Li, J. Cui, Y. Lei, Ammonia gas sensor using polypyrrole-coated TiO₂/ZnO nanofibers, Electroanalysis 21 (2009) 1432–1438.

[187] L. Su, W. Jia, A. Schempf, Y. Lei, Palladium/titanium dioxide nanofibers for glycerol electrooxidation in alkaline medium, Electrochem. Commun. 11 (2009) 2199–2202.

[188] W. Wang, P. Serp, P. Kalck, J.L. Faria, Photocatalytic degradation of phenol on MWNT and titania composite catalysts prepared by a modified sol–gel method, Appl. Catal. B: Environ. 56 (2005) 305–312.

[189] W. Wang, P. Serp, P. Kalck, J.L. Faria, Visible light photodegradation of phenol on MWNT-TiO$_2$ composite catalysts prepared by a modified sol–gel method, J. Molec. Catal. A: Chem. 235 (2005) 194–199.

[190] W. Wang, P. Serp, P. Kalck, C.G. Silva, J.L. Faria, Preparation and characterization of nanostructured MWCNT-TiO$_2$ composite materials for photocatalytic water treatment applications, Mater. Res. Bull. 43 (2008) 958–967.

[191] B. Gao, C. Peng, G.Z. Chen, G.L. Puma, Photo-electro-catalysis enhancement on carbon nanotubes/titanium dioxide (CNTs/TiO$_2$) composite prepared by a novel surfactant wrapping sol–gel method, Appl. Catal. B: Environ. 85 (2008) 17–23.

[192] B. Gao, G.Z. Chen, G.L. Puma, Carbon nanotubes/titanium oxide (CNTs/TiO$_2$) nanocomposites prepared by conventional and novel surfactant wrapping sol–gel methods exhibiting enhanced photocatalytic activity, Appl. Catal. B:Environ. 89 (2009) 503–509.

[193] X.H. Xia, Z.J. Jia, Y. Yu, Y. Liang, Z. Wang, L.L. Ma, Preparation of multi-walled carbon nanotube supported TiO$_2$ and its photocatalytic activity in the reduction of CO$_2$ with H$_2$O, Carbon 45 (2007) 717–721.

[194] A. Kongkanand, R.M. Dominguez, P.V. Kamat, Single wall carbon nanotube scaffolds for photoelectrochemical solar cells. Capture and transport of photogenerated electrons, Nano Lett. 7 (2007) 676–680.

[195] R. Bashyam, P. Zelenay, A class of non-precious metal composite catalysts for fuel cells, Nature 443 (2006) 63–66.

[196] M.-F. Manuel, V. Neburchilov, H. Wang, S.R. Guiot, B. Tartakovsky, Hydrogen production in a microbial electrolysis cell with nickel-based gas diffusion cathodes, J. Power Sources 195 (2010) 5514–5519.

[197] P.A. Selembo, M.D. Merril, B.E. Logan, Hydrogen production with nickel powder cathode catalysts in microbial electrolysis cells, Int. J. Hydrogen Energy 35 (2010) 428–437.

[198] K.-M. Lee, C.-Y. Hsu, P.-Y. Chen, M. Ikegami, T. Miyasaka, K.-C. Ho, Highly porous PProDOT-Et$_2$ film as counter electrode for plastic dye-sensitized solar cells, Phys. Chem. Chem. Phys. 11 (2009) 3375–3379.

[199] K.-M. Lee, P.-Y. Chen, C.-Y. Hsu, J.-H. Huang, W.-H. Ho, H.-C. Chen, K.-C. Ho, A high performance counter electrode based on poly(3,4-alkylenedioxythiophene) for dye-sensitized solar cells, J. Power Sources 188 (2009) 313–318.

[200] S. Ahmad, J.H. Yum, Z. Xianxi, M. Gratzel, H.J. Butt, M.K. Nazeeruddin, Dye-sensitized solar cells based on poly (3,4-ethylendioxythiophene) counter electrode derived from ionic liquids, J. Mater. Chem. 20 (2010) 1654–1658.

[201] M. Antoniadou, P. Lianos, Photoelectrochemical oxidation of organic substances over nanocrystalline titania: Optimization of the photoelectrochemical cell, Catal. Today 144 (2009) 166–171.

[202] M. Pagliaro, R. Ciriminna, H. Kimura, M. Rossi, C.D. Pina, From glycerol to value-added products, Angew. Chem. Int. Ed. 46 (2007) 4434–4440.

[203] A. Patsoura, D.I. Kondarides, X.E. Verykios, Photocatalytic degradation of organic pollutants with simultaneous production of hydrogen, Catal. Today 124 (2007) 94–102.

[204] A.A. Nada, H.A. Hamed, M.H. Barakat, N.R. Mohamed, T.N. Veziroglu, Enhancement of photocatalytic hydrogen production rate using photosensitized TiO$_2$/RuO$_2$-MV^{2+}, Int. J. Hydrogen Energy 33 (2008) 3264–3269.

[205] L.S. Al-Mazroai, M. Bowker, P. Davies, A. Dickinson, J. Greaves, D. James, L. Millard, The photocatalytic reforming of methanol, Catal. Today 122 (2007) 46–50.

[206] B. Kraeutler, A.J. Bard, Heterogeneous photocatalytic synthesis of methane from acetic acid-New Kolbe reaction pathway, J. Am. Chem. Soc. 100 (1978) 2239–2240.

[207] B. Kraeutler, A.J. Bard, Heterogeneous photocatalytic decomposition of saturated carboxylic acids on TiO$_2$ powder. Decarboxylative route to alkanes, J. Am. Chem. Soc. 100 (1978) 5985–5992.

[208] M. Antoniadou, D.I. Kondarides, P. Lianos, Photooxidation products of ethanol during photoelectrochemical operation using a nanocrystalline Titania anode and a two compartment chemically biased cell, Catal. Lett. 129 (2009) 344–349.

[209] P. Panagiotopoulou, M. Antoniadou, D.I. Kondarides, P. Lianos, Aldol condensation products during photocatalytic oxidation of ethanol in a photoelectrochemical cell, Appl. Catal. B: Environ. 100 (2010) 124–132.

[210] O.K. Varghese, C.A. Grimes, Appropriate strategies for determining the photoconversion efficiency of water photoelectrolysis cells: a review with examples using Titania nanotube array photoanodes, Sol. Energy Mater. Sol. Cells 92 (2008) 374–384.

[211] Y. Yu, P.V. Kamat, M. Kuno, A CdSe Nanowire/Quantum dot hybrid architecture for improving solar cell performance, Adv. Funct. Mater. 20 (2010) 1464–1472.

[212] H. Chang, X. Lv, H. Zhang, J. Li, Quantum dots sensitized graphene: in situ growth and application in photoelectrochemical cells, Electrochem. Commun. 12 (2010) 483–487.

[213] M. Miyake, H. Yoneyama, H. Tamura, Two step oxidation reactions of alcohols on an illuminated rutile electrode, Chem. Lett. 6 (1976) 635–640.

[214] Y. Maeda, A. Fujishima, K. Honda, The investigation of current doubling reactions on semiconductor photoelectrodes by temperature change measurements, J. Electrochem. Soc. 128 (1981) 1731–1734.

[215] M. Zhou, N.R. de Tacconi, K. Rajeshwar, Preparation and characterization of nanocrystalline composite (nanocomposite) films of titanium dioxide and nickel by occlusion electrodeposition, J. Electroanal. Chem. 421 (1997) 111–120.

[216] N.R. de Tacconi, H. Wenren, D. McChesney, K. Rajeshwar, Photoelectrochemical oxidation of formate ions on nickel-titanium dioxide nanocomposite electrodes: Unusually high "current doubling" yields and manifestation of a site proximity effect, Langmuir 14 (1998) 2933–2935.

[217] T. Ohno, S. Izumi, K. Fujihara, Y. Masaki, M. Matsumura, Vanishing of current-doubling effect in photooxidation of 2-propanol on TiO$_2$ in solutions containing Fe(III) ions, J. Phys. Chem. B 104 (2000) 6801–6803.

[218] P.A. Mandelbaum, A.E. Regazzoni, M.A. Blesa, S.A. Bilmes, Photo-electrooxidation of alcohols on titanium dioxide thin film electrodes, J. Phys. Chem. B 103 (1999) 5505–5511.